UC Riverside
UC Riverside Electronic Theses and Dissertations

Title

The Effects of Changing Water Chemistry on the Stability of Lead Service Lines

Permalink

https://escholarship.org/uc/item/1xm3q29p

Author

Orta, John Edward

Publication Date

2019

Copyright Information

Peer reviewed|Thesis/dissertation

UNIVERSITY OF CALIFORNIA
RIVERSIDE

The Effects of Changing Water Chemistry on the Stability of Lead Service Lines

A Thesis submitted in partial satisfaction
of the requirements for the degree of

Master of Science

in

Chemical and Environmental Engineering

by

John Edward Orta

December 2019

Thesis Committee:
    Dr. Haizhou Liu, Chairperson
    Dr. Brian Wong
    Dr. Cesunica Ivey

The Thesis of John Edward Orta is approved:

Committee Chairperson

University of California, Riverside

Acknowledgements

ABSTRACT OF THE THESIS

The Effects of Changing Water Chemistry on the Stability of Lead Service Lines

by

John Edward Orta

Master of Science, Graduate Program in Chemical and Environmental Engineering
University of California, Riverside, December 2019
Dr. Haizhou Liu, Chairperson

Lead-containing plumbing materials are widely used in drinking water systems across the globe. Being a toxic heavy metal, the release of lead within the drinking water distribution systems poses a major threat to public health. This study examined lead(II) mineral phases present in typical drinking water distribution systems by utilizing chemical equilibrium modeling. The predominant lead(II) minerals were exposed to free chlorine, a residual disinfectant, to study their oxidative transformation. In the absence of phosphate, cerussite $PbCO_{3(s)}$ and hydrocerussite $Pb_3(CO_3)_2(OH)_{2(s)}$ are the predominant phases, dependent on pH. The addition of phosphate induced the precipitation of pyromorphite $Pb_5(PO_4)_3Cl(s)$, lowering the total dissolved lead concentrations. The lead phosphate minerals resisted oxidation by chlorine, but the lead carbonate minerals reacted readily. The resulting solids were analyzed with XAS and revealed the generation of plattnerite $\beta\text{-}PbO_{2(s)}$ as the dominant Pb(IV) mineral, with trace amounts of scrutinyite $\alpha\text{-}PbO_{2(s)}$. Bromine oxidation of these Pb(II) minerals resulted in oxidation rate constants up to an order of magnitude greater than with chlorine. Using the derived rate constants, models of drinking water distribution systems were developed to show in the impact of bromide contamination. Although the lead(IV) phosphate minerals resisted oxidation, the

presence of bromide indicated these systems would be oxidized within a century. Next, the mobility of toxic metals in an oxidized system was investigated. Vanadinite $Pb_5(VO_4)_3Cl$ is present in systems with vanadium contamination and has the potential to release both vanadium and lead if oxidation occurs. Like the lead(II) phosphates, vanadinite resists chlorine oxidation but can be oxidized by bromine. This oxidation causes to the release of both lead and vanadium over time. Vanadium is very mobile, as almost 80% that passes through the 0.2 μm filter also passes through the 0.025 μ m filter. Lead is release occurs in the 0.2 μm filter but is effectively removed by the 0.025 μ m filter. This study provides fundamental understanding of lead surface chemistry in drinking water as well as strategies to prevent toxic metal release in drinking water distribution systems.

Table of Contents

List of Figures

Appendix

Chapter One

Introduction

1.1 Toxicity and regulations of lead

Lead is a heavy metal that is known to have toxic and detrimental effects on humans.[1-5] High blood lead levels (BLLs) have been shown to be fatal to humans. Elevated BLLs are associated with reduced fertility, elevated blood pressure and neurobehavioral effects in adults. In children, lead has been associated with decreased IQ scores, depressed vitamin D, and depressed hemoglobin. As such, there is no BLL that is considered safe in human children or adults. As a result, human lead exposure has been kept to a minimum through various regulations. This includes the Lead and Copper Rule (LCR), which established a drinking water maximum containment level (MCL) of 15 ppb, and the Toxic Substances Control Act (TSCA) section 403, which established hazardous lead levels in paint, dust and soils.

1.2 Human exposure to lead

Historically, there have been many sources for lead exposure including air, soil, gasoline, food and water. Although there have been government measures to reduce new sources of lead exposure, legacy contamination is still the major source for human exposure to lead. Currently, there is an estimated 6.1 million lead service lines (LSLs), lead-containing pipes, servicing 22 million people in the United States.[6] These pipes risk the exposure of lead in the drinking water distributed to residents, as was shown in both the Washington D.C[7] and Flint water crises.[8] Superfund sites are also major contributors to lead exposure. In these locations, lead from historical mining and smelting processes

has contaminated soil, rivers, and lakes, making these areas unsafe for human activity. Lead exposure can happen though inhalation, ingestion, and dermal absorption[9], making all situations of lead exposure dangerous.

1.3 Control strategies for lead release

The most effective strategy for preventing lead exposure is abatement. Removal of lead products from use guarantees minimum exposure. This includes removing lead-based paints, gasoline, and pipes from use and replacing them with safer alternatives. However, this is not possible in all cases due to the large financial burden associated with removing lead fixtures, particularly LSLs that can cost $2000 per pipe to replacement.[10] In these cases, controlling lead solubility by changing the water chemistry is the main method of preventing lead exposure. At typical drinking water conditions, cerussite [$PbCO_3$], is an expected lead mineral with relatively high solubility. Increasing pH of the water is a simple way to decrease the solubility by promoting hydrocerussite [$Pb_3(CO_3)_2(OH)_2$] formation. However, this rarely reaches the MCL by itself. Carbonate adjustment is used in tandem with pH adjustment to minimize lead solubility, typically in the ranges of 1-8mg C/L at a pH of 8.8-10.[11] The most widespread method of decreasing lead solubility is through the addition of orthophosphate to drinking water. Lead readily forms hydroxylpyromorphite [$Pb_5(PO_4)_3OH$] and chloropyromorphite [$Pb_5(PO_4)_3Cl$] in the presence of orthophosphate. These minerals have solubilities much lower than lead carbonates, under much broader pH ranges, meaning there is a broader application for orthophosphate addition. Deposition of a protective film on the pipe surface is the final

2

method for preventing lead release in LSLs. This can be done using silicates or calcium carbonate to form silicate and calcium carbonate protective films respectively.

1.4 Toxic Metal Accumulation in Lead Service Lines

Aside from lead being toxic to humans, other toxic metals and metalloids have been known to accumulate in lead minerals. Vanadium is of particular interest for lead service lines because it forms the complex mineral vanadinite, $Pb_5(VO_4)_3Cl$, and has been shown to coexist in has been found moderate concentrations within lead service lines.[12] Vanadium has been shown to cause decreased fertility, embryolethality, fetotoxicity, and teratogenicity.[13] This accumulated vanadium can pose a risk to human health if it is released into the drinking water.

1.5 Statement of the Problem

Water scarcity and climate change on a global level are causing a shift in drinking water chemistry. Techniques such as water reclamation and desalinization of sea water are being utilized to combat water scarcity but have vastly different chemical makeups when compared to traditional surface water or ground water treated for drinking water. In addition, anthropogenic causes, such as fracking, continue to pollute natural waters. One contaminant, bromide, has been shown to catalyze oxidation rates of metals in the presence of chlorine. These changes can cause a shift in lead chemical equilibrium, leading to a possible release event of toxic metals. This research is aimed at understanding the fundamental lead chemistry in drinking water distribution systems and modeling lead reactivity and release to prevent any health hazards that may occur from changing water chemistry.

Chapter 2

Understanding Lead Chemistry in Drinking Water Distribution Systems

2.1 Abstract

Lead-containing plumbing materials are widely present in drinking water distribution systems and they poses a continuing threat to public health. This study first examined lead(II) mineral phases in drinking water distribution systems using chemical equilibrium modeling. Predominant lead(II) minerals were then exposed to free chlorine, a residual disinfectant, to examine its effects on the oxidative transformation of lead(II) minerals. The effect of bromide on lead(II) oxidation was also investigated via bromine oxidation kinetics. The chemical equilibrium model predicted that in the absence of phosphate, lead(II) carbonate minerals including cerussite $PbCO_{3(s)}$ and hydrocerussite $Pb_3(CO_3)_2(OH)_{2(s)}$ are the predominant phases depending on solution pH. The presence of phosphate induces the formation of lead(II) phosphate mineral $Pb_5(PO_4)_3Cl_{(s)}$ in distribution systems, and results in an extremely low solubility. Advanced surface analysis using EXAFS and EXNES showed that the oxidation of lead(II) minerals generated plattnerite β-$PbO_{2(s)}$ as the primary Pb(IV) solid phases, with trace amounts of scrutinyite α-$PbO_{2(s)}$. Both lead(II) carbonate and phosphate minerals exhibited orders of magnitude higher oxidation rates with bromine than chlorine. Using reaction rate constants derived from these experiments and typical bromide levels in drinking water, we predict that systems not protected with phosphate will take up to 3 years to oxidize, accelerated to a few months in the presence of bromide. The presence of phosphate helps

to eliminate oxidation with free chlorine, but the presence of bromide can cause oxidation within a century. This study provides insightful understanding on the lead surface chemistry in drinking water and strategies to prevent lead release from drinking water infrastructure.

2.2 Introduction and Background

Lead (Pb) is a toxic metal harmful to human health when ingested waterborne. Lead poisoning retards mental capabilities in children at low exposure doses,[1,2] and causes organ failure at high exposure levels.[3,4] Lead has been used as a common plumbing material in drinking water distribution systems.[10] Even though the instillation of pure lead pipes has been halted since 1986, lead-containing brass and tine solder are still in use, which release Pb in drinking water distribution systems upon corrosion.[11-15] To combat waterborne lead-induced public health risks, a maximum contaminant level (MCL) of 15 µg/L for total lead in drinking water was established by the US EPA's Lead and Copper Rule (LCR).[16] However, lead release is still an issue in drinking water. For example, abrupt changes in drinking water chemistry can disrupt lead corrosion scales and equilibrium in distribution systems, resulting in dissolution of lead corrosion scales.[17-19] One example is the 2014-2017 lead crisis in Flint, Michigan. During that time, phosphate addition was stopped, leading to an abrupt change in water chemistry and a rapid release of lead above the MCL, in some homes surpassing the hazardous waste value of 5000 µg/L.[20,21] Similarly, in early 2000s of Washington DC, a change in disinfectant from chlorine to chloramine released toxic levels of lead from drinking water distribution systems.[22]

To control lead release, it is critical to understand the formation of lead minerals and associated chemistry. It has been known that lead(II) and lead(IV) are two relevant redox species in drinking water distribution systems. Lead(II) carbonate minerals including cerussite $PbCO_{3(s)}$ and hydrocerussite $Pb_3(CO_3)_2(OH)_{2(s)}$ are among the most commonly observed lead minerals in the corrosion scales.[23] However, lead concentrations in equilibrium with these minerals can exceed the limit placed by the LCR. Phosphate (PO_4^{3-}) addition is widely used to promote the formation of lead(II) phosphate minerals, *e.g.*, pyromorphite $Pb_5(PO_4)_3Cl_{(s)}$ and hydroxylpyromorphite $Pb_5(PO_4)_3OH_{(s)}$, which have much lower solubilities than the lead(II) carbonate minerals. Additionally, in drinking water with a high hardness level, calcium has been shown to substitute lead to form phosphohedyphane $Pb_3Ca_2(PO_4)_3Cl_{(s)}$ that also has very low solubility. Pb(II) minerals can be oxidized to Pb(IV) as lead dioxide $PbO_{2(s)}$ in the presences of residual disinfectant free chlorine.[11,21,26]

However, there is still deficiency in the understanding of speciation and redox reactivities of different lead minerals relevant to drinking water distribution system. In particular, the effects of bromide on lead redox speciation remains largely unknown. Elevated bromide levels in drinking water is a major concern, as bromide is introduced into the distribution system via the integration and blending of alternative water resources including recycled and desalinated water to meet rising water demands.[27-29] In addition, discharge of bromide containing wastes in coal-fired power utilities and hydraulic fracturing wastewaters are predicted to raise bromide levels by up to 20 times the current levels.[30] Bromide has been shown to catalyze chlorine oxidation through the formation of

hypobromous acid (HOBr). HOBr then becomes the *de facto* oxidant and it exhibits much higher reaction rates with the relevant Pb(II) minerals than free chlorine.[31-33] Furthermore, the kinetics of reactions involving the solid transformation of Pb(II) minerals remain unknown. Prior studies mostly measured free chlorine consumption rates to quantify the oxidation reaction kinetics.[11,13,28] There lacks a quantitative understanding on the direct Pb(IV) formation rates. A pursuit of this valuable knowledge is extremely important to establish lead solid phase transformation behavior and predict both solubility and mobility of lead in distribution systems.

The objectives of this study were to predict the predominant lead minerals under typical drinking water chemical conditions, including varying pH, alkalinity, chloride, calcium, and phosphate concentration, examine the oxidative transformation of lead(II) minerals with residual disinfectant free chlorine, investigate the effects of bromide on the chlorine oxidation reaction, and directly quantify the reaction kinetics involving solid phase transformation from lead(II) to lead(IV) minerals.

2.3 Methods and Materials

Select lead minerals including $Pb_3(CO_3)_2(OH)_{2(s)}$, $PbCO_{3(s)}$, and $\beta\text{-}PbO_{2(s)}$ were purchased from Sigma-Aldrich. Lead(II) phosphate minerals were synthesized using standard precipitation methods[34] and confirmed by X-ray diffraction (XRD). In brief, for $Pb_5(PO_4)_3OH_{(s)}$ synthesis, $NH_4H_2PO_4$ was quickly added to a solution of $PbNO_3$, and the pH of the stirred mixture was adjusted to 7.5 using NH_4OH. Then the solution was aged at 100°C for 48 hours. Synthesis of $Pb_5(PO_4)_3Cl_{(s)}$ followed a similar procedure with an

extra step of NaCl addition into the $NH_4H_2PO_4$ solution. Lead(II)-calcium mixed phase phosphate mineral – *i.e.*, phosphohedyphane $Pb_3Ca_2(PO_4)_3Cl$ – was synthesized based on established methods by Hopwood et. al.[25] The precipitated lead(II) minerals were separated using centrifugation and washed multiple times with deionized water to remove any residual ions. Samples were then freeze dried, ground and sieved a nominal size of 105 to 88 μm using mesh No. 140 and 170 sieves. Fresh free chlorine solutions were diluted from a 5% NaOCl stock solution. Bromine solutions were synthesized by adding 10% molar excess NaBr to a free chlorine solution and equilibrated for one hour.[35]

Evaluation on the predominant lead(II) mineral in different drinking water chemical conditions was conducted based on equilibrium chemistry using the software Geochemist's Workbench.[36] Equilibrium constants of all lead(II) species were obtained from the Visual MINTEQ database,[37] except that the solubility product of phosphohedyphane was experimentally obtained and added to the software database (details provided in Text A.1).

To evaluate the oxidative transformation of lead(II) minerals, oxidation experiments were performed in well-mixed 250-mL flasks in the dark at 22 °C. A concentration of 5 g/L of lead(II) carbonate or phosphate minerals was mixed with excess chlorine at a molar ratio of 1 to 3. This initial concentration was chosen to quantify solid phase reaction kinetics, and they do not alter the redox reaction thermodynamics under drinking water chemical conditions. The solution pH was adjusted to 7 ± 0.5 and maintained by manual addition of 0.5 M $HClO_4$ or 0.5 M NaOH when needed. Samples were taken at pre-determined

intervals and filtered with a 0.1-µm filter. Retained solids were washed with 50 mL of DI water and freeze dried for speciation analysis.

Chlorine or bromine concentration in the filtered samples was analyzed using the standard DPD method.[38] Pb(II) and Pb(IV) solid speciation in the solid samples was directly quantified using X-ray absorption spectroscopy (XAS), including both X-ray absorption near edge spectroscopy (XANES) and extended X-ray absorption fine structure (EXAFS). Samples were measured using beamlines 11-2 and 4-1 at Stanford Linear Accelerator Center (SLAC) National Accelerator Laboratory. Before the XAS measurement, samples were grounded and diluted using boron nitride (BN) to reach an absorption length of 1.5. Data was collected from 12800 eV to 13925 eV for the lead L_{III} edge at 13035 eV using a scan time of 30 minutes, and the collected XAS spectra were analyzed using Athena software. Speciation fractionation was determined using linear combination in the XAS processing software Athena. This fitting consists of the mathematical combination of the multiple well-defined standard spectra to recreate the experimental spectra. Fitting required a R-factor ≤ 0.01 to ensure good fit between modeled and real results. Solid phase reaction kinetics were modeled using a second order reaction rate. Details on the data fitting of the kinetics rate constants were provided in Text A.2 of the appendix. The crystal structure of solid samples was analyzed via XRD using a PANalytical Empyrean Series 2 machine scanning from 10°-90°.

2.3 Results and Discussion

2.3.1 Effect of corrosion control strategies on lead(II) mineral speciation in drinking water.

The predominant lead(II) mineral in the corrosion scales of lead-containing drinking water distribution systems varies greatly based on the drinking water chemistry and the implementation of corrosion control strategies. In systems that use pH or alkalinity adjustments as the corrosion control strategy,[37] cerussite and hydrocerussite are the predominate phases of lead (Figure 2.1A). Under these conditions, *i.e.*, pH between 5 and 9, and alkalinity between 0 and 100 mg/L as $CaCO_3$, the solubility of lead ranges between 0.1 and 1 mg/L, exceeding the US EPA MCL of 15 µg/L at all relevant pH values. Another common lead corrosion control strategy in drinking water distribution system is the addition of phosphate.[37] Under chemical conditions with typical 0.5-2 mg/L of phosphate, pyromorphite $Pb_5(PO_4)_3Cl_{(s)}$ becomes the predominant mineral phase across all relevant pHs (Figure 2.1B). The solubility of pyromorphite is much lower than either cerussite or hydrocerussite, resulting in an equilibrated soluble lead level between 0.2 and 10 µg/L, which is well below the MCL of 15 µg/L. Increasing the chloride level continues to drop the solubility, but at a depreciated rate compared to phosphate (Figure A.1). These figures demonstrate that phosphate addition minimizes lead solubility in drinking water.
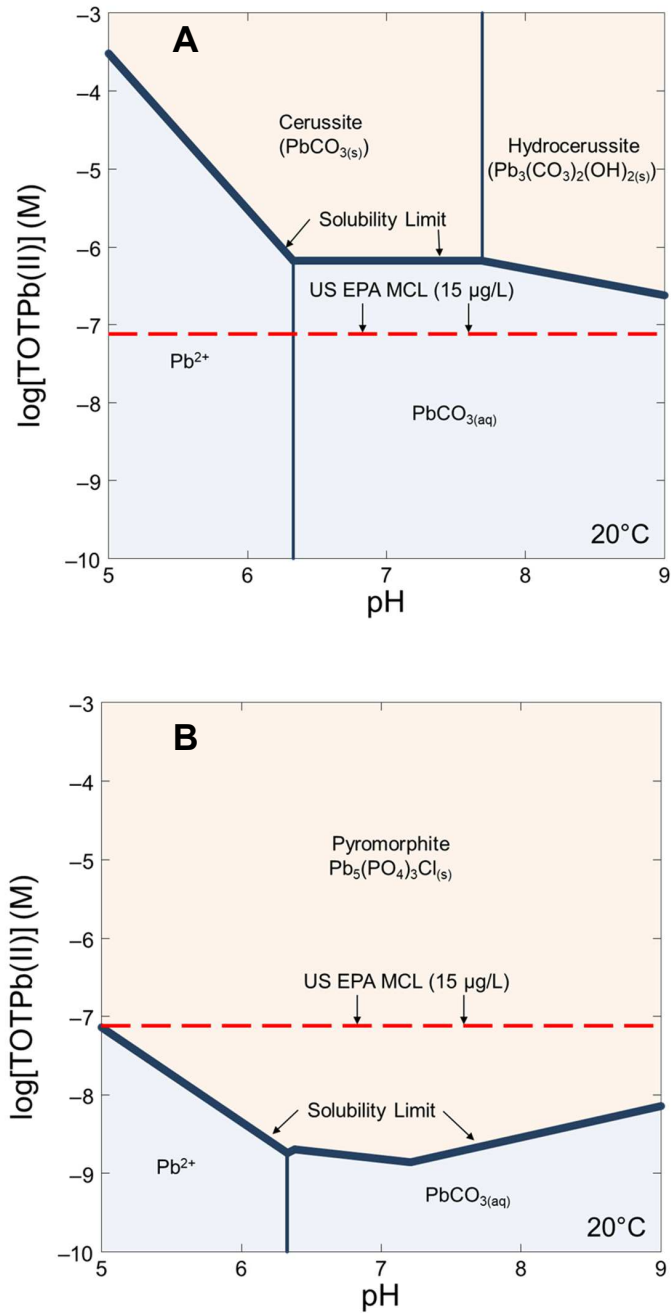
Figure 2.1 Equilibrium diagram for lead in common drinking water systems utilizing different control strategies. Bolded line represents the total dissolved Pb(II) concentration. Red dashed line represents the US EPA MCL for lead. T=20 °C, ionic strength=0.01M (a) TOTCO$_3$=1 mM, [Cl$^-$]=0.1 mM. (b) TOTCO$_3$=1 mM, [Cl$^-$]=0.1 mM, [PO4^{3-}] = 0.5 mg/L.

2.3.2 Effects of chlorine on lead mineral speciation in drinking water

Free chlorine, the most common of the disinfectants, possesses a redox potential that is thermodynamically favorable to covert Pb(II) minerals to Pb(IV) solids under typical drinking water chemical conditions (Table S1). For example, the oxidation of cerussite by free chlorine proceeds as following:

$$PbCO_{3(s)} + HOCl + H_2O \rightarrow PbO_{2(s)} + H^+ + Cl^- + H_2CO_3 \qquad \text{(Reaction 2.1)}$$
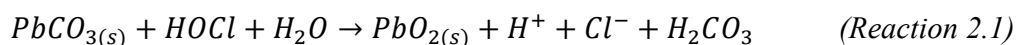
The XANES data showed that $PbCO_{3(s)}$ was transformed to $PbO_{2(s)}$ via chlorine oxidation (Figure 2.2A). The formation of a pre-edge Pb(IV) shoulder at 13030 eV and a post-edge Pb(IV) peak at 13060 eV indicated an oxidative transformation of Pb(II) to Pb(IV). Linear combination fitting of the XANES data showed that the solid phase oxidation of $PbCO_{3(s)}$ followed a *pseudo* first-order reaction kinetics, and 80% of $PbCO_{3(s)}$ was converted to $PbO_{2(s)}$ after 120 minutes of reaction (Figure 2.2B). A second-order reaction rate constant of 3.9×10^{-3} $M^{-1}s^{-1}$ was calculated for $PbCO_{3(s)}$ oxidation by chlorine (Table 2.1). XRD analysis confirmed the Pb(IV) phase as plattnerite β-$PbO_{2(s)}$ (Figure A2). Similarly, $Pb_3(CO_3)_2(OH)_{2(s)}$ was readily oxidized by free chlorine to $PbO_{2(s)}$ based on XANES data analysis (Figure 2.3A), with 95% solid phase conversion to $PbO_{2(s)}$ within 120 minutes (Figure 2.3B). A second-order reaction rate constant of 1.0×10^{-2} $M^{-1}s^{-1}$ was calculated for $Pb_3(CO_3)_2(OH)_{2(s)}$ oxidation by chlorine (Table 2.1). In contrast, $Pb_5(PO_4)_3Cl_{(s)}$ and $Pb_5(PO_4)_3OH_{(s)}$ showed much less reactivity with free chlorine than lead(II) carbonate minerals, with no noticeable oxidative solid phase transformation after 5 days of reaction based on XANES data (Figures A3-A5). XRD analysis also showed no
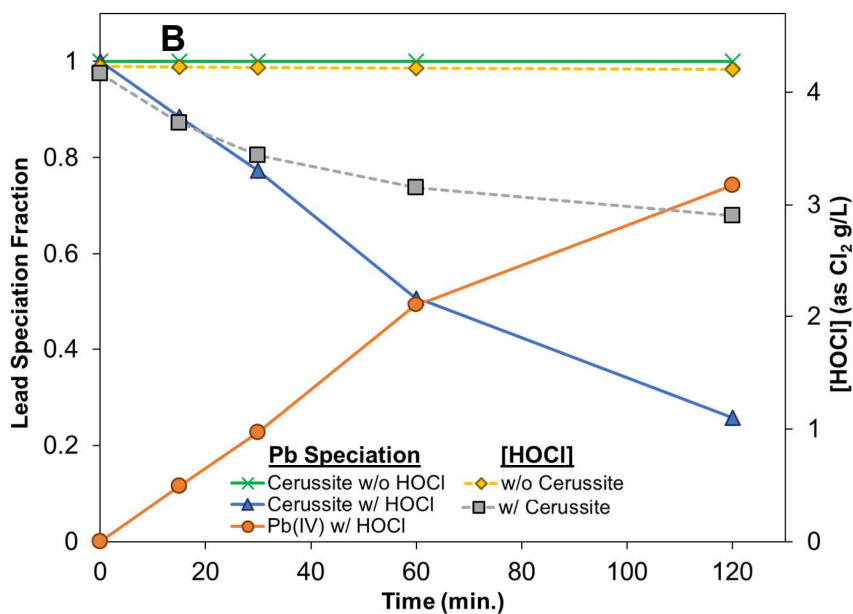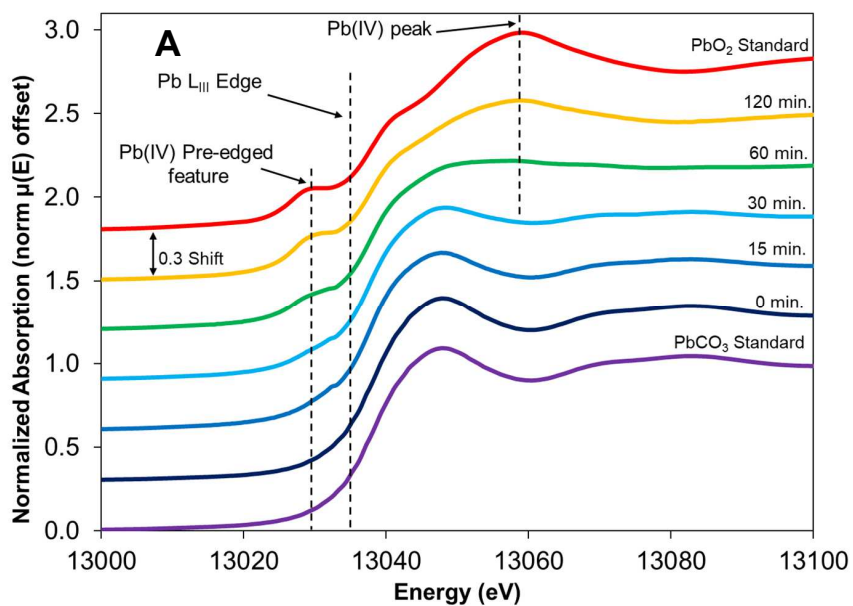
Figure 2.2 Cerussite oxidation by HOCl. $TOTCO_3 = 10$ mM, $[HOCl]_0 = 4.2$ g/L as Cl_2, initial $Cl_2:Pb(II)=3:1$, $T=22°C$, pH=7 (a) XANES of cerussite oxidation; $[PbCO_3]_0 = 5$ g/L (b) Lead speciation in cerussite oxidation.

conversion of $Pb_5(PO_4)_3OH_{(s)}$ (Figure A5). This is consistent with previous literature that hydroxylpyromorphite was resistant to oxidation by chlorine when compared to the carbonate species.[33]

Effects of bromide on lead mineral speciation in drinking water

As cities begin to incorporate desalinated water and reclaimed water as their new water sources in the future to combat climate impact on diminishing fresh water resources, bromide levels are expected to increase.[35-37] With increased bromide, free bromine is generated in drinking water systems due to the transformation of free chlorine by bromide:

$$HOCl + Br^- \rightarrow HOBr + Cl^- \qquad \textit{(Reaction 2.2)}$$
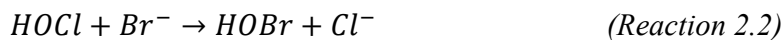
Free bromine is thermodynamically capable of oxidizing Pb(II) minerals to Pb(IV) solids under realistic drinking water chemical conditions (Table A1). For example, the reaction of cerussite with free bromine is as following:

$$PbCO_{3(s)} + HOBr + H_2O \rightarrow PbO_{2(s)} + H^+ + Br^- + H_2CO_3 \quad \textit{(Reaction 2.3)}$$
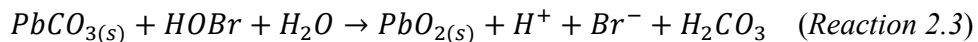
Therefore, to evaluate the effects of bromide, we first conducted bromine oxidation experiments on representative lead(II) solid phases. The oxidation of $Pb_3(CO_3)_2(OH)_{2(s)}$ by bromine also generated $PbO_{2(s)}$, (Figure 2.4A). However, the rate was much faster than chlorine oxidation, reaching over 95% of conversion to in only 30 minutes (Figure 2.4B).
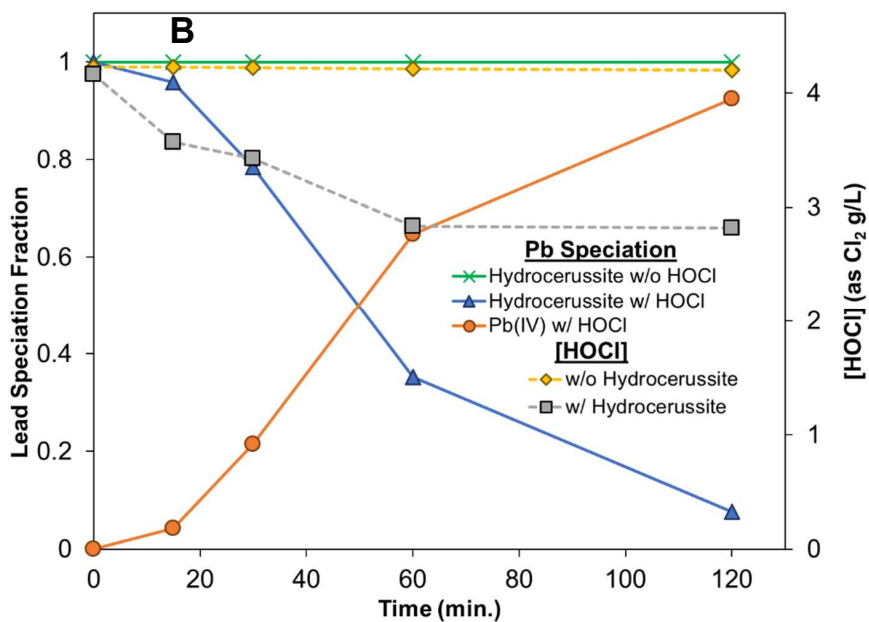
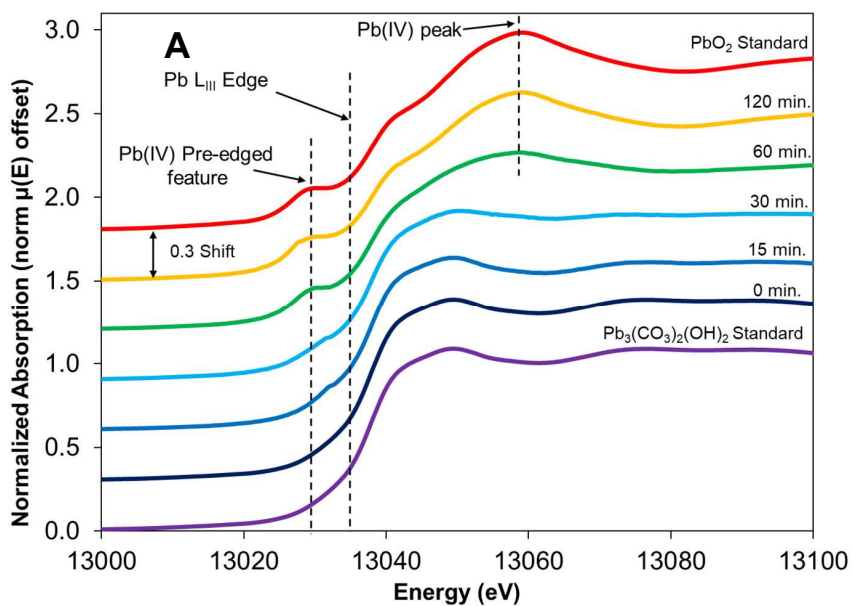**Figure 2.3** Hydrocerussite oxidation by HOCl. $TOTCO_3$ = 10 mM, $[HOCl]_0$ = 4.2 g/L as Cl_2, initial Cl_2:Pb(II)=3:1, T=22°C, pH=7 (a) XANES hydrocerussite of oxidation; $[Pb_3(CO_3)_2(OH)_2]_0$ = 5.0 g/L (b) Lead speciation in hydrocerussite oxidation.

The calculated reaction rate for $Pb_3(CO_3)_2(OH)_{2(s)}$ oxidation by bromine is 6.1×10^{-2} $M^{-1}s^{-1}$ (Table 2.1). Cerussite behaved similarly, with over 95% oxidative conversion to β-$PbO_{2(s)}$ in 30 minutes (Figures A6-A7) and a calculated reaction rate constant of 4.7×10^{-2} $M^{-1}s^{-1}$ (Table 2.1). Free bromine exhibited reaction rates *ca.* 6-12 times greater than chlorine for cerussite and hydrocerussite oxidation, respectively. Furthermore, compared to chlorine, bromine oxidized a significant fraction of $Pb_5(PO_4)_3Cl_{(s)}$ minerals (Figures 2.5A and 2.5B). In 7 hours of reaction, approximately 20% of $Pb_5(PO_4)_3Cl_{(s)}$ was oxidized to Pb(IV). The oxidation rate constant was calculated as 8.4×10^{-4} $M^{-1}s^{-1}$ (Table 2.1). $Pb_5(PO_4)_3OH_{(s)}$ also exhibited significant oxidation in the presence of bromine, with 10% oxidation within 7 hours and a calculated reaction rate of 1.6×10^{-4} $M^{-1}s^{-1}$ (Figure A8 and Table 2.1). XRD confirmed that bromine oxidation product from these two reactions was confirmed as β-$PbO_{2(s)}$ as well (Figure A9). These data suggested that bromide impacted reaction kinetics of oxidative Pb(II) solid phase transformation, but not the final Pb(IV) product. The catalytic behavior of bromide on redox reaction was also observed in prior studies involving transition metals and metalloids.[33]

Stoichiometry of lead(II) solid phase oxidation by chlorine and bromine

The ratio between the amount of Pb(II) consumed was compared against the amount of oxidant consumed (Figure 2.6). Based on reactions 1 and 3, a ratio of 1:1 is expected between all minerals and oxidants. For the carbonate minerals, a ratio of *ca.* 1 is observed. However, with the phosphate minerals, the ratios are much lower, at 0 for chlorine and close to 0.2 for bromine oxidation, far from the ideal ratio of 1. One
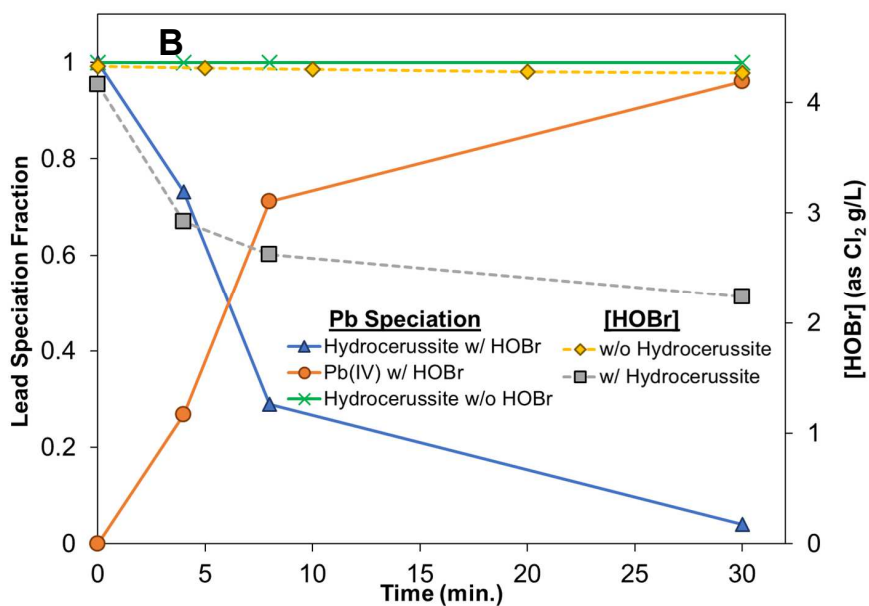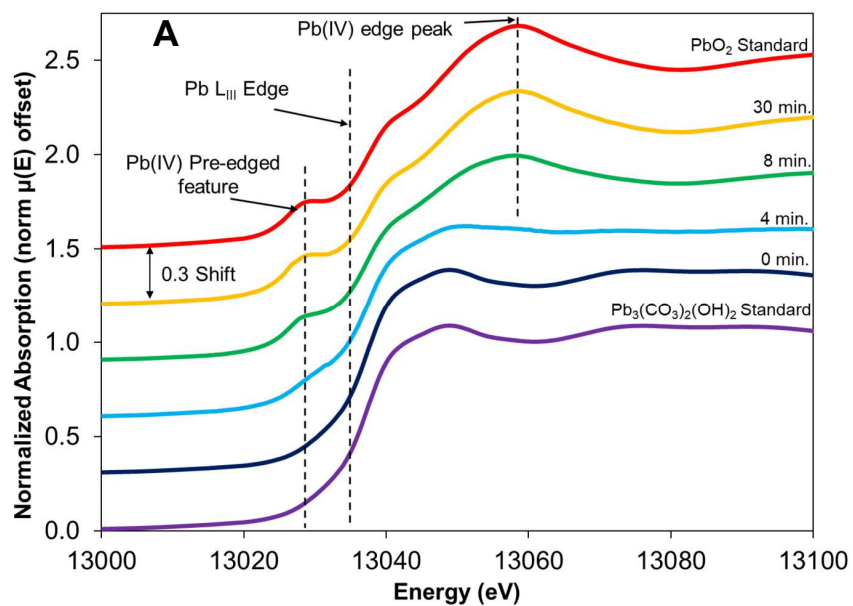
Figure 2.4 Hydrocerussite oxidation by HOBr. (a) XANES of hydrocerusite oxidation; $[PbCO_3]_0 = 5$ g/L (b) Lead speciation in hydrocerussite oxidation.

Table 2.1 Second-order rate constant for lead minerals with respective oxidant

Mineral	2nd order rate constant (M^{-1}s^{-1})	
	HOCl	HOBr
Cerussite	3.9×10^{-3}	4.7×10^{-2}
Hydrocerussite	1.0×10^{-2}	6.1×10^{-2}
Pyromorphite	-	8.4×10^{-4}
Hydroxylpyromorphite	-	1.8×10^{-4}

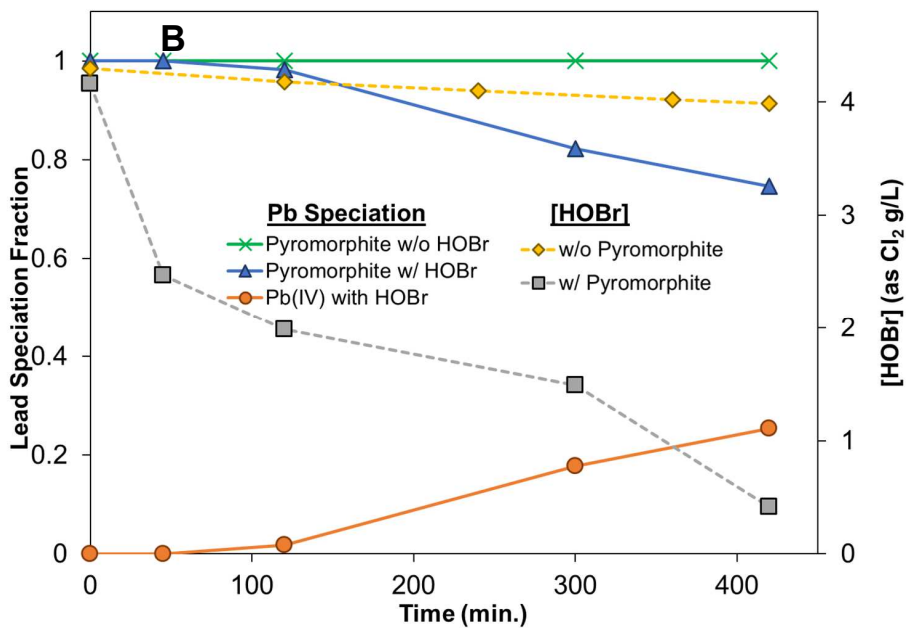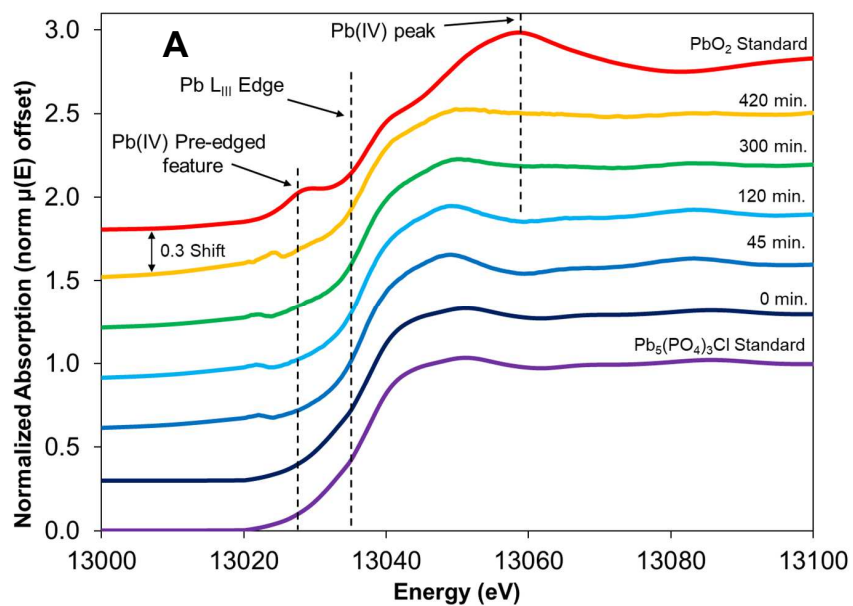**Figure 2.5** Pyromorphite oxidation by HOBr. (a) XANES of pyromorphite oxidation; $[Pb_5(PO_4)_3Cl]_0 = 5$ g/L (b) Lead speciation in pyromorphite oxidation.
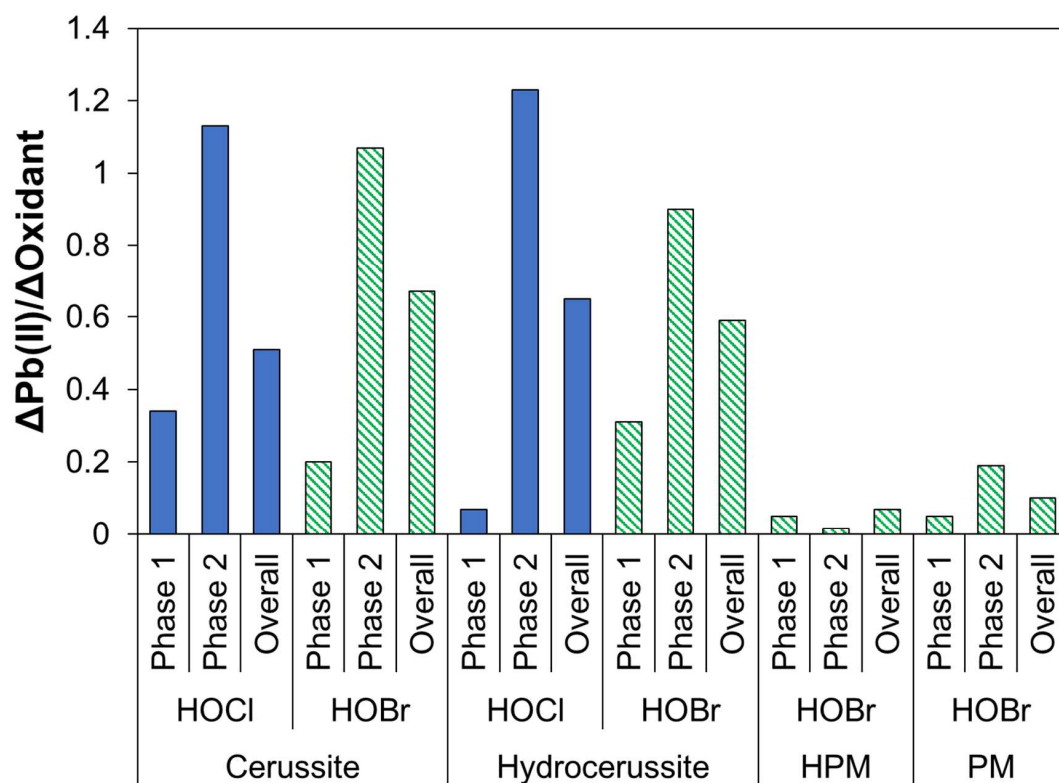
Figure 2.6 Ratio between Pb(II) and oxidant consumed during various phases of Pb(II) oxidation by free chlorine and free bromine. Stoichiometric ratio between Pb(II) and both oxidants is 1:1. HPM = Hydroxylpyromorphite, PM = Pyromorphite.

explanation for this is the formation of Pb(III) intermediates that rapidly decay back to Pb(II) and release oxygen, as shown below.

$$\text{HOCl} \xrightarrow[Pb(III)O^*]{Pb(II)} \frac{1}{2} O_2 + H^+ + Cl^- \qquad\qquad (\textit{Reaction 4})$$
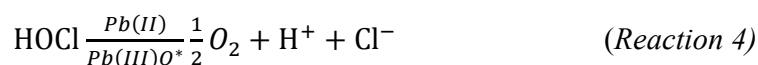
Reaction 3 shows that free chlorine has an autocatalytic decay in the presence of Pb(II) solids. This means that unstable Pb(III) solids facilitate the decomposition of chlorine to chloride and oxygen when the complete oxidation to Pb(IV) is too slow. Additional experimental data shows that oxygen generated from this reaction can help to account for the chlorine consumption not related to Pb(II) conversion.

Environmental Implications

Using the calculated *pseudo* first-order reaction rates, oxidation of Pb(II) minerals in drinking water distribution systems can be predicted. For example, a LSL with a residual chlorine level of 0.5 mg/L is examined with varying bromide concentrations. Details on the calculation are shown in Text A3 in the SI. For a drinking water distribution systems dominated with cerussite as the corrosion scales, having only free chlorine present would take over 3 years for 90% of the present Pb(II) to be transformed to Pb(IV). The introduction of as of bromide reduces that time to under a year (Figure 2.7). Generally, the oxidation of Pb(II) to Pb(IV) solids is encouraged, as it further decreases the solubility of lead. This conversion is beneficial to the minimization of lead solubility. For the lead(II) phosphate minerals, oxidation takes place at a much slower rate. At the higher bromide concentrations of 3 mg/L, pyromorphite would take over 60 years to reach 90% oxidations. Although long, this can reasonably happen within the lifetime of the pipes, as

21

pipes in water infrastructure have been known to be used for over 100 years. These values show that a change in water chemistry in water distribution systems can shift an equilibrium that takes years, if not decades, to stop being reactive.

Conclusion

Lead release in public water supplies is a health problem that needs to be addressed. By understanding its chemical equilibrium and solid phases, the release of lead in drinking water can be mitigated. Since phosphate addition is the most effective and most used method of lead corrosion control in drinking water distribution systems, this work offers a better understanding to the formation of minerals within the corrosion scales and how these minerals interact with the water matrix. This work shows that pyromorphite will be the dominant lead mineral phase in lead systems that have been treated with phosphate. This suggests that a more focused study into the interactions of lead phosphate minerals is the key to understanding lead stability in drinking water. This work also shows the importance of bromine oxidation of lead by free chlorine, as the formation of bromine due to elevated bromide in drinking water can greatly increase the solid transformation rates of Pb(II) to Pb(IV).

By understanding this transformation of Pb(II) minerals to PbO_2, much can be seen told about lead levels in water. When looking at the solubility of lead, PbO_2 has the lowest solubility, leading to the lowest level of dissolved lead. However, the lower solubility of lead does not mean lower lead levels in general. Other factors, such as NOM, may induce
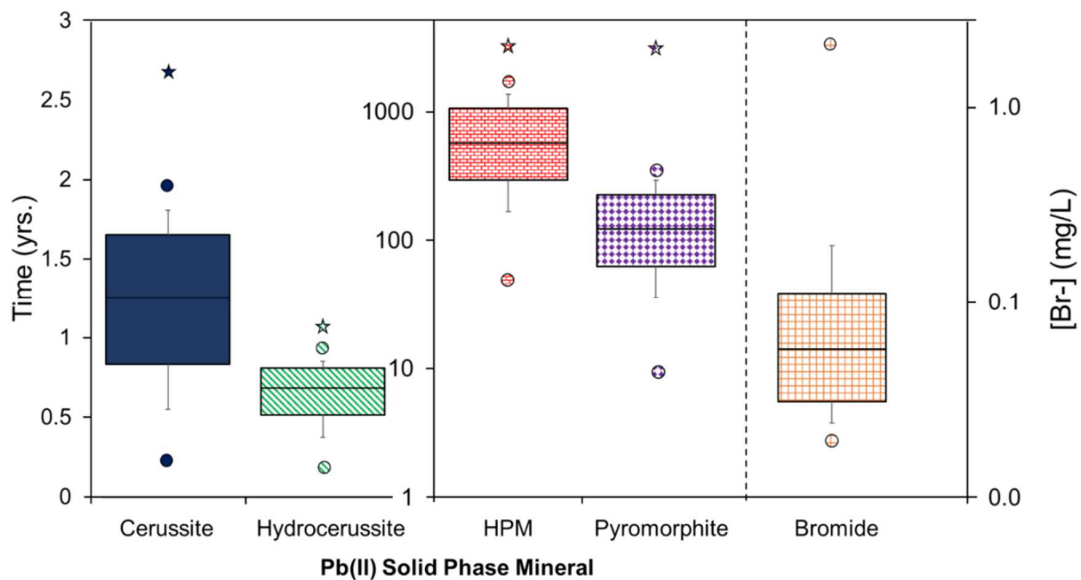
Figure 2.7 Time required to oxidize 90% of different Pb(II) minerals to Pb(IV) in water distribution systems utilizing free chlorine in the presence of varying bromide concentrations. HPM= Hydroxylpyromorphite. pH = 7, T = 22°C, $[\text{Oxidant}]_{ss}$ = 0.5 mg/L as Cl_2. Dots represent the minimum and maximum predicted bromide concentrations, whiskers represent 95% and 5% distributions, lines represent the 1st, 2nd, and 3rd quartile of bromide distribution, and star represents 0 mg/L Br^-.

colloidal mobilization of $PbO_{2(s)}$, leading to higher overall lead exposure.[42-44] Further

research is needed to conclude if oxidation leads to higher or lower lead levels overall.

Chapter Three

Release of Toxic Metals in Drinking Water Distribution Systems

3.1 Purpose

The purpose of chapter three is to understand how lead oxidation effects toxic metal release, particularly lead and vanadium. Understanding of reactivity and the transport of these toxic metals is vital to preserving human health in areas that are exposed to these dangers in their drinking water systems.

3.2 Methods and Materials

$Pb_5(VO_4)_3Cl$ was synthesized using a well-established method and confirmed using XRD. A 14 mM free chlorine solution was prepared from a 5% NaOCl solution. A 14 mM bromine (HOBr) stock solution was prepared by mixing free chlorine and NaBr with 15% molar excess of the latter for one hour. In each experiment, a targeted dosage of one Pb(II) solid with 2.1 mM of total Pb was added into a completely mixed batch reactor. The dosage of chlorine or bromine was controlled at a value of 50 mg L^{-1} as Cl_2. This gives a Cl_2:Pb ratio of 1:3 to ensure complete oxidation of chlorine. This concentration was also chosen to develop a kinetic model that is still relevant under typical drinking water conditions. The ratio was later flipped to 3:1 by reducing the total lead to 0.23 mM to reduce noise and scattering detected in the ICP-MS. The solution pH was maintained at targeted values between 7.0 and 10 using a Eutech Instrument Alpha pH200 controller with 50 mM $HClO_4$ and 50 mM NaOH, which did not interfere with lead redox chemistry and have been widely used for pH control purposes. All experiments were conducted at 22°C in the dark. At pre-determined time intervals,

samples were taken from the Pb(II)/oxidant suspension and sequentially filtered using 0.2μm, and 0.025μm Millipore filters. The filtered samples were analyzed for chlorine or bromine concentration using the standard DPD method. Samples were then analyzed using ICP-MS to determine total concentrations of V and Pb.

3.3 Results and Discussion

3.3.1 Effects of pH on Vanadinite Oxidation

Vandinite is predicted to react with oxidants in a similar way to the pyromorphite series. As such, the oxidation of vanadinite is modeled by the following reaction:

$$Pb_5(PO_4)_3Cl_{(s)} + 5HOBr + 5H_2O \rightarrow 5PbO_{2(s)} + 6H^+ + 5Br^- + Cl^- + H_3VO_4$$
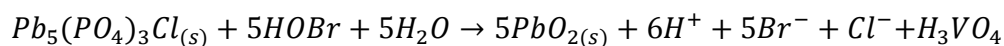
(Reaction 3.1)

The consumption of bromine was monitored to establish the oxidation kinetics of vanadinite. Free bromine was the oxidant of choice, as lead minerals in this family are resistant to free chlorine oxidation as shown in previous data. Vanadinite oxidation was measured from pH 7 to pH 10 at intervals of 0.5 to span most relevant drinking water conditions. Figure 3.1 shows the relationship between oxidant consumption and pH. As seen in the graph, there is very little variation in oxidation rates across the chosen pH range. Previous studies have shown that an increase in pH leads to a decrease in kinetic oxidation rate due to the transformation of HOCl and HOBr to the less electrophilic species OCl⁻ and OBr⁻, respectively. These results suggest that vanadinite has complexes that form across the range of pH's tested which cause it to have an increased reactivity. These two processes bring balance to the overall oxidation rate of vanadinite.
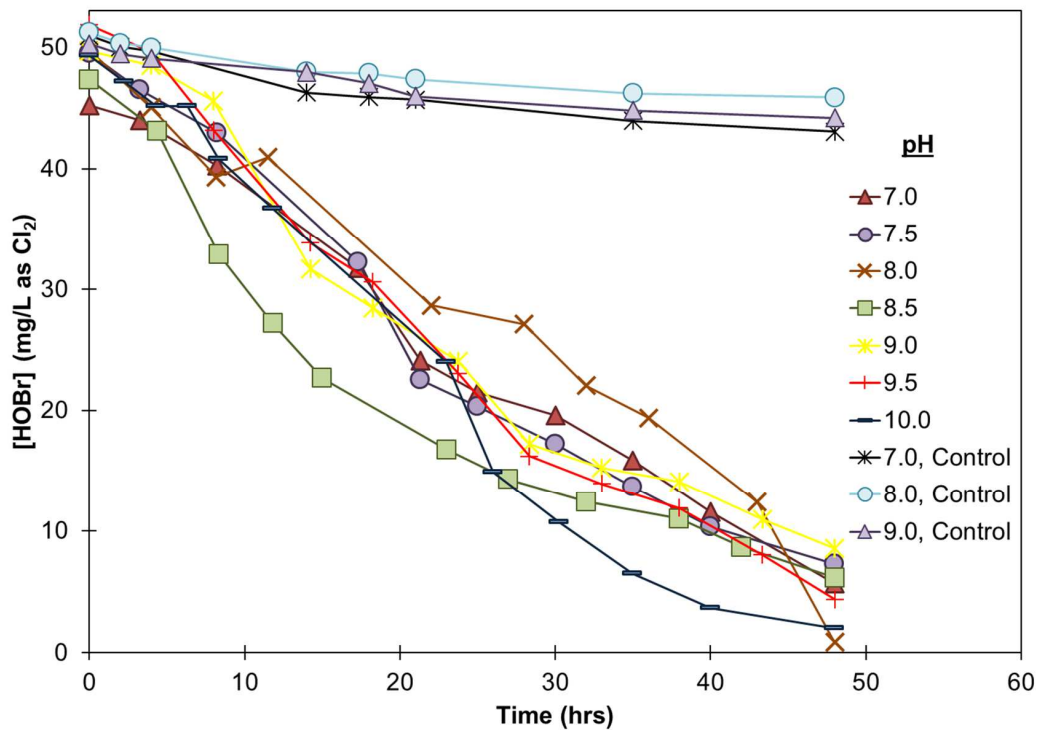
Figure 3.1 Bromine consumption profiles for the oxidation of vanadinite by free bromine. T= 22°C, TOTCO$_3$= 1 mM, IS= 10 mM, [Pb$_5$(VO$_4$)$_3$Cl]=0.595 g/L, intial [HOBr]= 50 mg/L as Cl$_2$
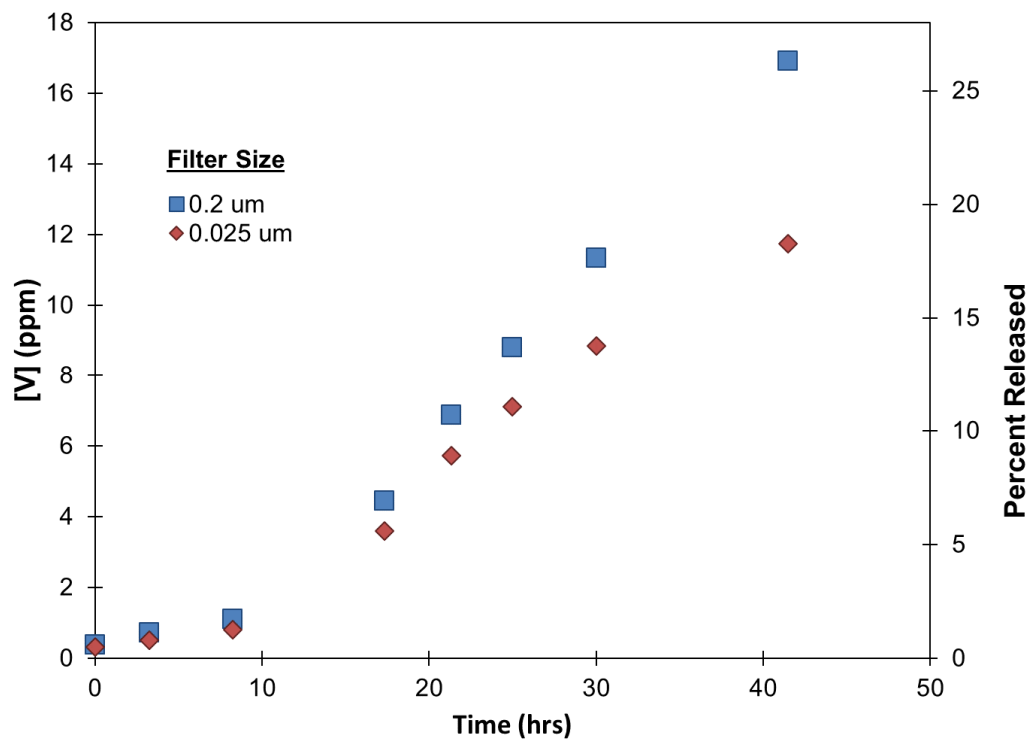
Figure 3.2 Vanadium release from the oxidation of $Pb_5(VO_4)_3Cl$ by HOBr. pH= 7, T= 22°C, $TOTCO_3$= 1 mM, IS= 10 mM, $[Pb_5(VO_4)_3Cl]$=0.595 g/L, intial [HOBr]= 50 mg/L as Cl_2

3.3.2 Toxic Metal Release

Both vanadium and lead concentrations were monitored to track changes of toxic metals released into the water caused by the oxidation of vanadinite. Samples were sequentially filtered through 0.2μm and 0.025μm Millipore filters to see the fractionation between sizes. It is to note that 0.2μm is below the normally recognized "dissolved" filter size of 0.45μm. Figure 3.2 shows vanadium concentrations through the 0.2μm filter continually increased over time until the completion of the reaction. This accounts for over 25% of the total vanadium added to the system. Under complete oxidation, an expected 33% would have been released. When sequentially filtered through the 0.025μm filter, vanadium levels decrease to 70%-80% of the value obtained from the 0.2μm filter throughout the entire process. Both observations are key to understanding vanadium release. First, since the vanadium concentrations continuously increase while bromine is constantly consumed, it is shown that vanadium release is a direct result of $Pb_5(VO_4)_3Cl$ oxidation. The second is that most of the vanadium is completely dissolved in the water, as most of it passed through both filters. This helps to confirm the release of vanadium as its soluble form, not forming any other unknown solid. This means that if a release event occurred, filtration would be an ineffective way of trying to reduce vanadium levels. When looking at lead concentrations through the 0.2μm filter, the release over time is much more scattered, but still shows a general trend of increasing over time (Figure 3.3). However, the lead concentrations through the smaller 0.025μm filter show a much different trend. Here, lead levels decrease substantially, at some points the concentration is less that 0.5% of the value originally reported from the 0.2μm filter. This is a
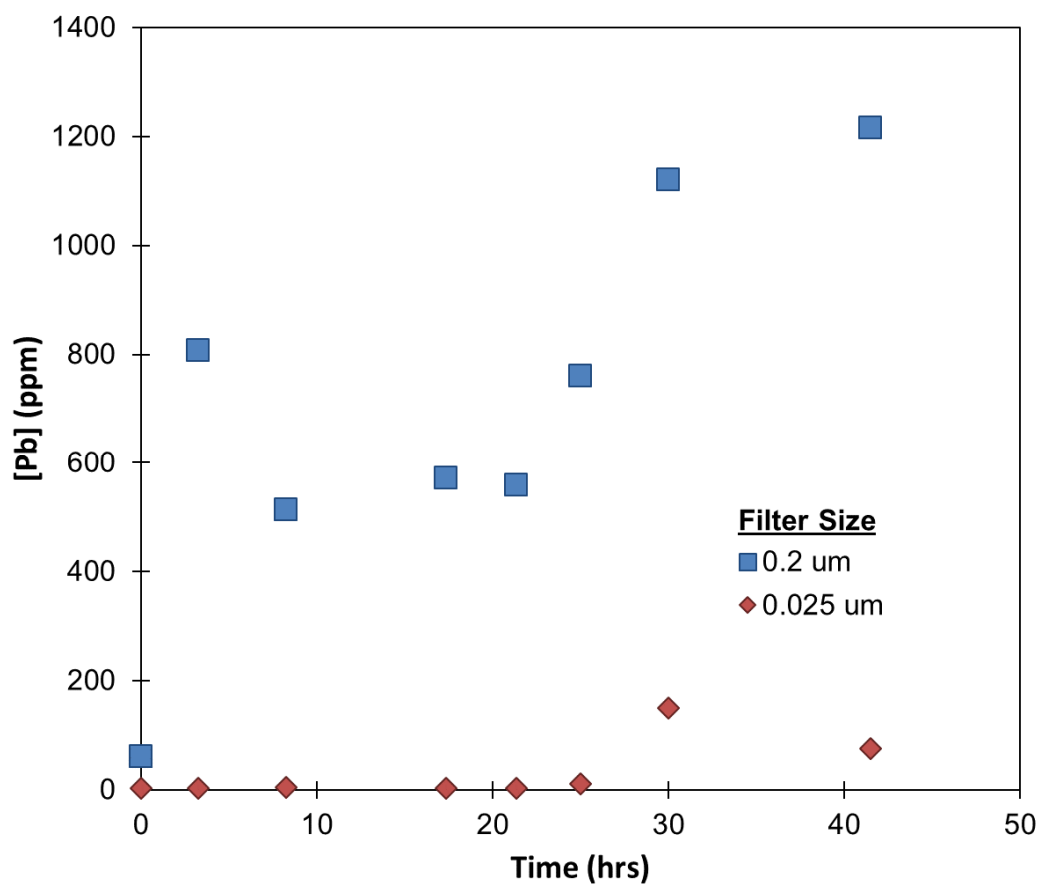
Figure 3.3 Lead release from the oxidation of $Pb_5(VO_4)_3Cl$ by HOBr. pH= 7, T= 22°C, $TOTCO_3$= 1 mM, IS= 10 mM, $[Pb_5(VO_4)_3Cl]$=0.595 g/L, intial [HOBr]= 50 mg/L as Cl_2
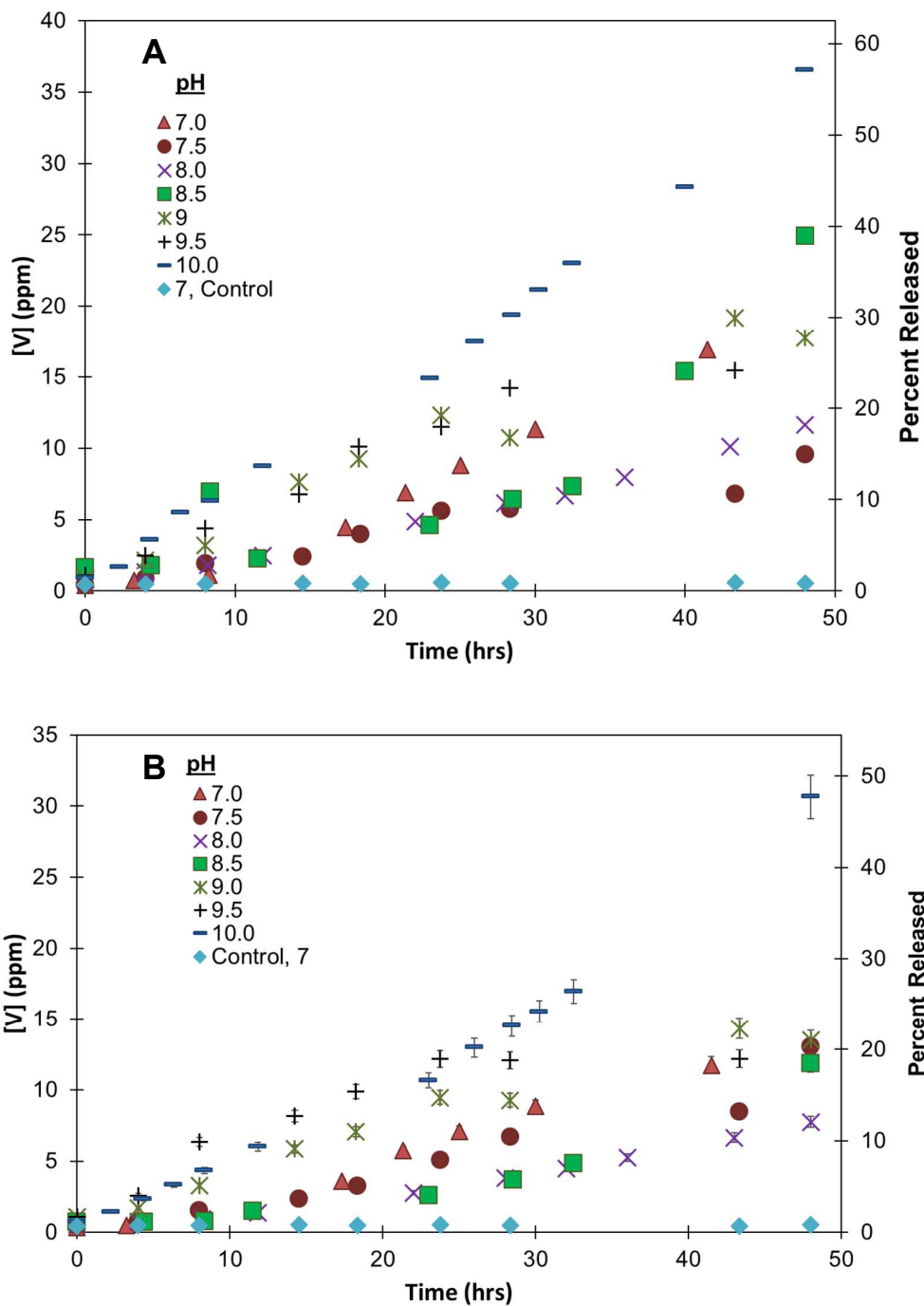
Figure 3.4 Vanadium release from the oxidation of $Pb_5(VO_4)_3Cl$ by HOBr across varying pH. T= 22°C, $TOTCO_3$= 1 mM, IS= 10 mM, $[Pb_5(VO_4)_3Cl]$=0.595 g/L, intial [HOBr]= 50 mg/L as Cl_2. (a) 0.2μm filter. (b) 0.025μm filter.

substantial observation, as this shows that most lead exposure is through larger colloids that can be filtered out.

Next, the effects of pH on vanadium and lead release were studied. As with before, vanadium concentrations shows a consistent increase over time. However, vanadium concentrations vary depending on pH. Total vanadium concentrations decrease from pH 7 to pH 8 but increase from pH 8 to the maximum concentrations at pH 10 (Figure 3.4A and B). Sequential filtration through the 0.025μm filter showed that 70%-80% of the vanadium that passed through the 0.2μm filter passed through the smaller filter. The total release of vanadium also reaches a maximum of 59%, almost double the expected 33% from complete consumption of the oxidant. This shows that on top of the oxidation releasing vanadium, the solubility of vanadium increases at the higher pH, leading to a higher overall vanadium level. This demonstrates that changes in water chemistry has great potential to release vanadium that has accumulated that is difficult to remove with just filtration. When looking at lead, the same general observations from before hold true. There is a general increase of lead concentrations over time, but it is very scattered (Figure 3.5A and B). Again, there is a major reduction of lead levels when passed through the smaller filter, showing particulate formation as a major contributor of lead levels at all pH values.

3.4 Conclusions

This chapter provides great insight to the fate and transport of toxic metals during the oxidation of lead. Vanadium, a toxic metal that has been shown to accumulate in lead containing pipes, forms vanadinite $Pb_5(VO_4)_3Cl$ that, when oxidized, releases the
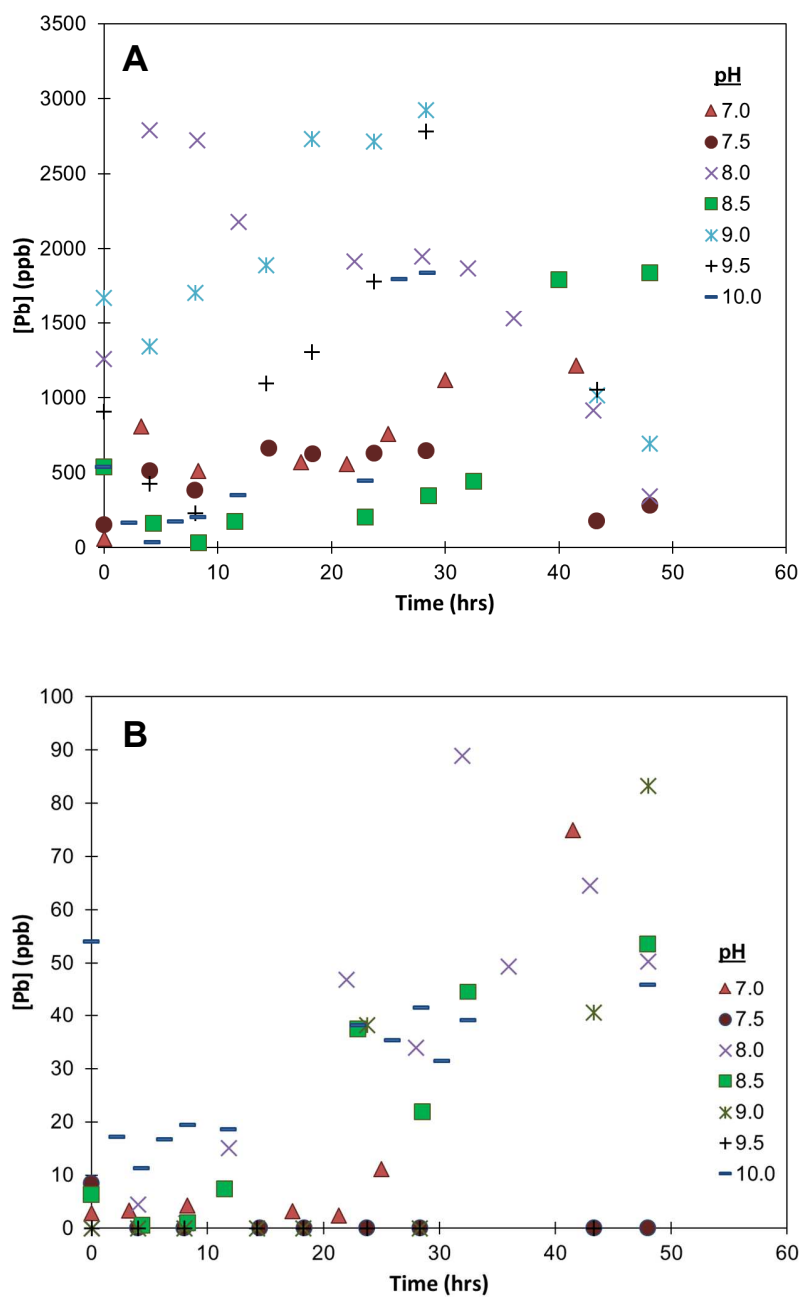
Figure 3.5 Lead release from the oxidation of $Pb_5(VO_4)_3Cl$ by HOBr across varying pH. T= 22°C, $TOTCO_3$= 1 mM, IS= 10 mM, $[Pb_5(VO_4)_3Cl]$=0.595 g/L, intial [HOBr]= 50 mg/L as Cl_2. (a) 0.2μm filter. (b) 0.025μm filter.

Chapter Four

4.1 Conclusions

Overall, this work aims to understand the fundamental chemistry behind lead and the minerals associated with lead in drinking water and the impact that climate change and water scarcity will have on the stability of lead. Through the use of solubility modeling, it was shown that cerussite and hydrocerussite are the governing minerals in systems not utilizing phosphate control. In the presence of phosphate, the pyromorphite family becomes the governing mineral due to its extremely low solubility. Vanadium, a toxic metal, has been shown to accumulate in lead pipes and form vanadinite, a lead and vanadium mineral. The lead carbonate minerals were then readily oxidized by free chlorine, a common disinfectant, while the pyromorphites resisted any oxidation. The implications of climate change and water scarcity will lead to the changing of water chemistry over time, which can include the increase in concentration of bromide entering water distribution systems. This bromide can act as a catalyst to the lead and free chlorine reaction, causing much more rapid oxidation of lead pipes. This oxidation can cause in increase in toxic metals, both lead and vanadium, that make it into the drinking water. While the lead forms particulates that can be filtered out using more extreme filter sizes, vanadium is completely soluble and requires greater lengths to prevent contamination. This research provides key understanding into lead chemistry, reactivity and the transport of toxic metals.

Works Cited

(1) Stokes, L.; Onwuche, N. C.; Thomas, P.; Davies-Cole, J. O. Blood lead levels in residents of homes with elevated lead in tap water—district of Columbia MMWR Morb. Mortal Wkly. Rep., **2004**, 53 (12), 268–270, 2004.

(2) Ferrie, J. P.; Rolf, K.; Troesken, W. Cognitive disparities, lead plumbing, and water chemistry: prior exposure to water-borne lead and intelligence test scores among World War Two U.S. Army enlistees. Econ. Hum. Biol. **2012**, 10 (1), 98–111.

(3) Gidlow, D.A., Lead toxicity Occup. Med. (Lond) 2004, 54(2), 76–81.

(4) Abadin, H.; Ashizawa, A.; Stevens, Y.W. Toxicological Profile for Lead, US Department of Health and Human Services, Agency for Toxic Substances and Disease Registry (ATSDR), Atlanta, Ga, USA, **2007**.

(5) Schwartz, J. Low-Level lead exposure and children's IQ: a meta-analysis and searching for a threshold. *Environ Res*. **1994**, 65, 42-55.

(6) McTigue, N. E.; Cornwell, D. A.; Graf, K.; Brown, R. Occurrence and consequences of increased bromide in drinking water sources'. Am. Water Works Assoc. **2014**, 106, E492−E508.

(7) US EPA. Elevated Lead in D.C. Drinking Water – A study of Potential Causative Events, Final Summary Report. **2007**, EPA 815-R-07-021

(8) Guidotti, T.L.; Calhoun, T.' Davies-Cole, J.O.; Knuckles, M.E.; Stokes, L.; Glymph, C.; Lum, G.; Moses, M.S.; Goldmsith, D.; Ragain, L. Elevated lead in drinking water in Washington, DC, 2003-2004: The public health response. *Environ Health Perspect*. **2007**, 115(5), 695-701.

(9) Qu, C.; Ma, Z.; Yang, J.; Liu, Y.; Bi, J.; Huang, L. Human Exposure Pathways of Heavy Metals in a Lead-Zinc Mining Area, Jiangsu Province, China. *PLOS One*. **2012**, 7(11).

(10) Renner, R. Reaction to the Solution: Lead Exposure Following Partial Service Line Replacement. *Environ Health Perspect*. 2010 May; 118(5): A202–A208.

(11) Shock, M. Understanding Corrosion Control Strategies for Lead. *J. Am. Water Work. Assn.* **1989**, 81(7), 88-100

(12) Shock, M.; Hyland, R.; Welch, M. Occurrence of Contaminant Accumulation in Lead Pipe Scales from Domestic Drinking-Water Distribution Systems. *Environ. Sci. & Technol.* **2008**, 42, 4285-4291.

(13) Doingo, J. Vanadium: A Review of the Reproductive and Developmental Toxicity. *Reproductive Toxicology*. **1996**, 10(3), 175-182

(14) U.S. Environmental Protection Agency. Prohibition on use of lead pipes, solder and flux. Available online: https://www.gpo.gov/fdsys/pkg/CFR-1999-title40-vol15/xml/CFR1999-title40-vol15-sec141-43.xml

 (15) Liu, H.; Korshin, G.V.; Ferguson, J.F. Interactions of Pb(II)/Pb(IV) solid phases with chlorine and their effects on lead release. Environ. Sci. & Technol. **2009**, 43 (9), 3278-3284.

(16) Liu, H.; Schonberger, K. D.; Korshin, G.V.; Ferguson, J.F.; Meyerhofer, P; Desormeaux, E.; Luckenbach, H. Effects of blending of desalinated water with treated surface drinking water on copper and lead release. Water Res. **2010**, 44 (14), 4057-4066.

(17) Kim, E. J.; Herrera, J. E. Characteristics of lead corrosion scales formed during drinking water distribution and their potential influence on the release of lead and other contaminants. Environ. Sci. Technol. **2010**, 44 (16), 6054–6061.

(18) Ng, D.-Q.; Strathmann, T. J.; Lin, Y.-P. Role of orthophosphate as a corrosion inhibitor in chloraminated solutions containing tetravalent lead corrosion product PbO2. Environ. Sci. Technol. 2012, 46 (20), 11062–11069.

(19) Triantafyllidou, S.; Schock, M. R.; DeSantis, M. K.; White, C. Low contribution of PbO2 - coated lead service lines to water lead contamination at the tap. Environ. Sci. Technol. 2015, 49 (6), 3746–3754.

(20) U.S. Environmental Protection Agency. Maximum contaminant level goals and national primary drinking water regulations for lead and copper. 1987 Available online: http://www.epa.gov/dwreginfo/lead-and-copper-rule 263–269,.

(21) Kim, E. J.; Herrera, J. E.; Huggins, D.; Braam, J.; Koshowski, S. Effect of pH on the concentrations of lead and trace contaminants in drinking water: A combined batch, pipe loop and sentinel home study. Water Res. 2011, 45 (9), 2763–2774.

(22) Del Toral, M. A.; Porter, A.; Schock, M. R. Detection and evaluation of elevated lead release from service lines: A field study. Environ. Sci. Technol. 2013, 47 (16), 9300–9307.

(23) Cantor, A. F.; Park, J. K.; Vaiyavatjamai, P. Effect of chlorine on corrosion in drinking water systems. J. Am. Water Work. Assn. 2003, 95, 112–123.

(24) Olson, T. M.; Wax, M.; Yonts, J.; Heidecorn, K.; Haig, S. J.; Yeoman, D.; Hayes, Z.; Raskin, L.; Ellis, B. R. Forensic Estimates of Lead Release from Lead Service Lines during the Water Crisis in Flint, Michigan. Environ. Sci. Technol. Lett. 2017, 4, 356.

(25) Pieper, K. J.; Tang, M.; Edwards, M. A. Flint water crisis caused by interrupted corrosion control: investigating "ground zero" home. Environ. Sci. Technol. 2017, 51 (4), 2007– 2014.

(26) Edwards, M.; Dudi, A. role of chlorine and chloramine in corrosion of lead-bearing plumbing materials. J. Am. Water Work. Assn. 2004, 96, 69–81.

(27) Liu, H.; Korshin, G.V.; Ferguson, J.F.; Jiang, W. Key parameters and kinetics of oxidation of lead (II) solid phases by chlorine in drinking water. Water Practice and Technology. 2006, 1 (4)

(28) Colling, J. H.; Whincup, P. A. E.; Hayes, C. R. The measurement of plumbosolvency propensity to guide the control of lead in tap waters. Water Environ. J. 2007, 1 (3), 263-269

(29) Hopwood, J. D.; Derrick, G. R.; Brown, D. R., et al. The identification and synthesis of lead apatite minerals formed in lead water pipes. J. Chem. 2016, https://doi.org/10.1155/2016/9074062

(30) Lytle, D.A; Schock, M.R. Formation of Pb(IV) oxides in chlorinated water. J. Am. Water Works Assoc. 2005, 97, 102-114.

(31) Taylor, J.; Dietz, J.; Randall, A.; Hong, S. Impact of RO-desalted water on distribution water qualities. Water Sci. Technol. 2005, 51 (6-7), 285-291
.
(32) Tang, Z.; Hong, S.; Xiao, W.; Taylor, J. Impacts of blending ground, surface, and saline waters on lead release in drinking water distribution systems. Wat. Res. 2006, 40 (5), 943-950.

(33) Magazinovic, R. S.; Nicholson, B. C.; Mulcahy, D. E.; Davey, D. E. Bromide levels in natural waters: its relationship to levels of both chloride and total dissolved solids and the implications for water treatment. Chemosphere. 2004, 57 (4), 329−335.

(34) S. Allard, L. Fouche, J. Dick, A. Heitz, U. von Gunten, Oxidation of Manganese (II) during Chlorination: Role of Bromide. Environ. Sci. Technol. 2013, 47, 8716-8723

(35) Orta, J.; Patton, S.; Liu, H. Bromide-Assisted Catalytic Oxidation of Lead(II) Solids by Chlorine in Drinking Water Distribution Systems. Chem. Commun. 2017, 53, 8695-8698.

(36) Farkas, L.; Lewin, M.; Bloch, R. The reaction between hypochlorite and bromides. J. Am. Chem. Soc. 1949, 71, 1988-1991.

(37) Zhu, Y.; Zhu, Z.; Zhao, X.; Liang, Y.; Huang, Y. Characterization, Dissolution, and solubility of lead hydroxylpyromorphite [Pb5(PO4)3OH] at 25-45°C. J. Chem. 2015, Article ID 269387, 10 pages.

(38) Jolley, R.L.; Carpenter, J. H. Aqueous chemistry of chlorine: Chemistry, analysis and environmental fate of reactive oxidant species. ORNL/TM 7788. Oak Ridge Natl. Lab. 1982.

(39) Geochemical and Biogeochemical Reaction Modeling, 564 p., Cambridge Press, 2008

(40) Gustafsson, J. P. Visual MINTEQ ver. 3.1. 2014

(41) Rice, E.; Baird, R.; Eaton, A.; Cleceri, L.; Standard Methods for the Examination of Water and Wastewater, American Public Health Association, Washington, DC, 22nd edn, 2012

(42) McNeill, L. S.; Edwards, M. Importance of Pb and Cu particulate species for corrosion control. J. Environ. Eng., 2004,130(2), 136–144.

(43) Triantafyllidou, S.; Parks, J.; Edwards, M. Lead particles in potable water, J. - Am. Water Works Assoc., 2007, 99(6), 107–117.

(44) Korshin, G.; Liu, H. Preventing the colloidal dispersion of Pb(IV) corrosion scales and lead release in drinking water distribution systems. Environ. Sci.: Water Res. Technol., 2019.

Table A1 Relevant reduction and oxidation equations with real reduction potential under real drinking water conditions. Ionic strength = 0.01M, [Cl⁻] = 35ppm, [Cl₂] = 0.62ppm, [PO₄³⁻] = 0.5mg/L, [Ca²⁺] = 40ppm, TOTCO₃ = 1mM, [Pb²⁺] = 0.01ppm, pH = 7.

Reaction	Redox Reactions	Standard E (V)	Actual E (V)
1	$5\beta\text{-}PbO_{2(s)} + 20H^+ + 10e^- + 3\ PO_4^{3-} + Cl^- \rightleftharpoons Pb_5(PO_4)_3Cl + 10\ H_2O$	3.82	-0.88
2	$5\beta\text{-}PbO_{2(s)} + 19H^+ + 10e^- + 3\ PO_4^{3-} \rightleftharpoons Pb_5(PO_4)_3OH + 9\ H_2O$	3.33	-1.16
3	$3\beta\text{-}PbO_{2(s)} + 12H^+ + 6e^- + 3\ PO_4^{3-} + Cl^- + 2Ca^{2+} \rightleftharpoons Pb_3Ca_2(PO_4)_3Cl + 6\ H_2O$	3.71	0.49
4	$\beta\text{-}PbO_{2(s)} + CO_3^{2-} + 4H^+ + 2e^- \rightleftharpoons PbCO_3 + 2\ H_2O$	1.85	0.84
5	$3\beta\text{-}PbO_{2(s)} + 2CO_3^{2-} + 10H^+ + 6e^- \rightleftharpoons Pb_3(CO_3)_2(OH)_2 + 4\ H_2O$	2.02	-0.41
6	$HOCl_{(aq)} + H^+ + 2e^- \rightleftharpoons Cl^- + H2O$	1.49	1.22
7	$HOBr_{(aq)} + H^+ + 2e^- \rightleftharpoons Br^- + H2O$	1.34	1.16

Text A1: Adding minerals to Geochemists WorkBench and choosing concentration ranges

Solubility experiments were run utilizing Phosphohedyphane $Pb_3Ca_2(PO_4)_3Cl$ to calculate solubility. A 1g/L solution of Phosphohedyphane was brought to a pH of 7 with an ionic strength of 10mM suing $NaClO_4$. The solution was continuously stirred, and samples were drawn then filtered through a 0.22 μM filter. Samples were then analyzed via ICP-MS to determine metal concentration, and Ion Chromatography for chloride concentrations. The following equation was used to calculate K_{sp}:

$$K_{sp} = (\gamma_{Pb}[Pb^{2+}])^3 * (\gamma_{Ca}[Ca^{2+}])^2 * (\gamma_{Cl}[Cl^-])$$

The activity coefficients were assumed to be 1, as ionic strength was low and constant. Phosphohydyphane was calculated to have a K_{sp} of 10^{-76} and was added to the database. Drinking water chemical parameters including pH, alkalinity, chloride, calcium, and phosphate concentration were varied to show effects on mineral formation. Alkalinity ($TOTCO_3$) and hardness were varied between 5 and 100 mg/L as $CaCO_3$, low hardness to upper end of soft water consideration. Orthophosphate level ranged between 0 and 2 mg/L as PO_4^{3-}, corresponding to no orthophosphate treatment and the upper limit of corrosion control dosage[i]. Chloride addition was varied from 3.55-250 mg/L, low chloride concentration to the secondary MCL set by the EPA[ii].

Text A2: Calculating Rate second order rate constants

Reaction between the Pb(II) minerals and oxidant (ie. chlorine and bromine) was assumed to be an elementary reaction. The reaction rate equation for Pb(II) with these oxidants is shown below:

$$\frac{dPb(II)}{dt} = -kC_{Pb(II)}C_{Ox} \qquad \text{(Equation 1)}$$

Where k is the second order reaction rate constant, $C_{Pb(II)}$ is the concentration of Pb(II), and C_{Ox} is the concentration of the respective oxidant. A moving average was used for the concentration of oxidant, as shown in equation 2:

$$\frac{dPb(II)}{dt} = -kC_{Pb(II)}C_{Ox_{avg}} \qquad \text{(Equation 2)}$$

Where $C_{Ox_{avg}} = \frac{C_{Ox_t} + C_{Ox_{t+1}}}{2}$. Numerical integration was performed for every time point and the resulting equation was solved for k.

$$k = -\frac{\ln(\frac{C_{Pb(II)t+1}}{C_{Pb(II)t}})}{C_{Ox_{avg}}\Delta t} \qquad \text{(Equation 3)}$$

Reaction rate constants for the rapid decay phase, defined as the reaction occurring after 5% oxidation of Pb(II) species, were averaged to obtain the second order ration rate constant. This rate constant was then optimized using a model to predict Pb(II) concentrations and compared to the experimental results. Fitting parameters were solved to include a local R^2 of 1 ± 0.05, local slope of 1 ± 0.1 and intercept of 0 ± 0.05.

Text A3: Modeling of distribution systems using representative concentrations

Drinking water distribution systems were modeled using kinetic coefficients derived from experimental data as described in text 3. Drinking water conditions were defined as follows: Ionic strength (IS) = 1mM, [Cl$_2$] = 0.5mg/L, pH = 7, T = 22°C. Any bromide present was assumed to react instantly with free chlorine, forming free bromine. Concentrations were assumed to be steady state for a flowing system. 90% conversion of Pb(II) solids to Pb(IV) was the target time frame. The system was modeled according to equation 4.

$$\frac{dPb(II)}{dt} = -k_{HOCl}C_{Pb(II)}C_{HOCl} - k_{HOBr}C_{Pb(II)}C_{HOBr} \qquad \text{(Equation 3)}$$

Where k_{HOCl} is the second order rate constant for each Pb(II) mineral with free chlorine, k_{HOBr} is the second order rate constant for each Pb(II) mineral with free bromine, $C_{Pb(II)}$ is the concentration of Pb(II) minerals, C_{HOCl} is the concentration of free chlorine, and C_{HOBr} is the concentration of free bromine. Integration and solving of the equation yields the following equation:

$$\ln\left(\frac{C_{Pb(II)t}}{C_{Pb(II)0}}\right) = -(k_{HOCl}C_{HOCl} + k_{HOBr}C_{HOBr})\Delta t \qquad \text{(Equation 4)}$$

Where $C_{Pb(II)0}$ is the initial concentration of Pb(II), $C_{Pb(II)t}$ is the concentration at time t, and Δt is the elapsed time. Assuming 90% conversion, $\ln\left(\frac{C_{Pb(II)t}}{C_{Pb(II)0}}\right)$ can be substituted with $\ln(0.1)$ and the equation solved for Δt to get total time for oxidation of Pb(II) solids.
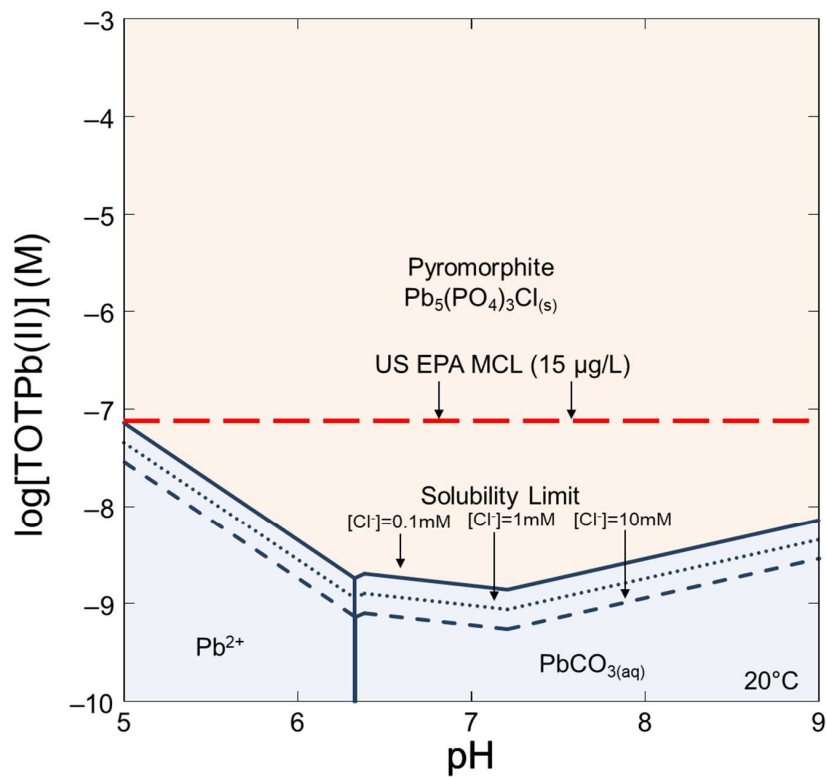
Figure A1 Equilibrium diagram for lead in common drinking water systems utilizing different control strategies. Bolded line represents the total dissolved Pb(II) concentration. Red dashed line represents the US EPA MCL for lead. T = 20°C, IS = 0.01M, $TOTCO_3$ = 1 mM, $[Cl^-]$ = 1 mM, $[PO_4^{3-}]$ = 0.5 mg/L
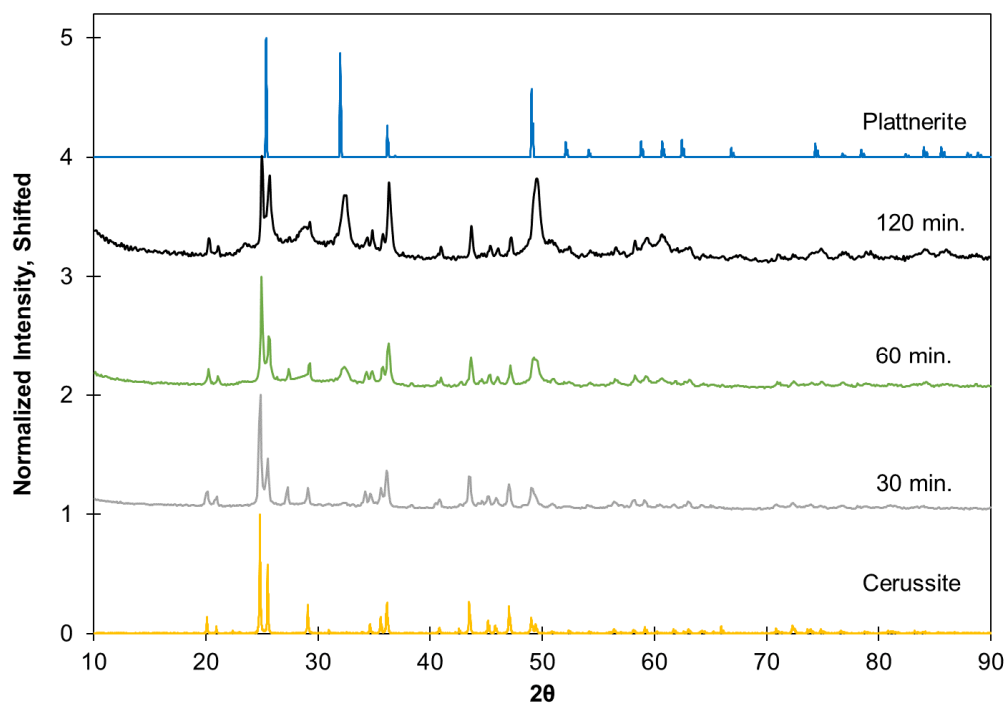
Figure A2 XRD spectra of lead solids during cerussite oxidation by free chlorine. $TOTCO_3$ = 10 mM, $[HOCl]_0$ = 4.2 g/L as Cl_2, initial $Cl_2:Pb(II)$=3:1, T=22°C, pH=7.
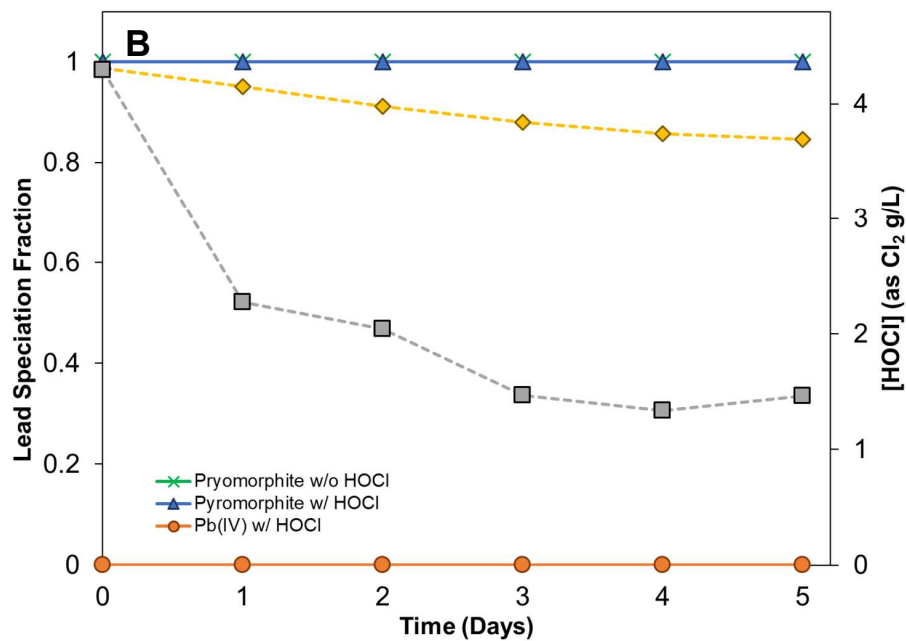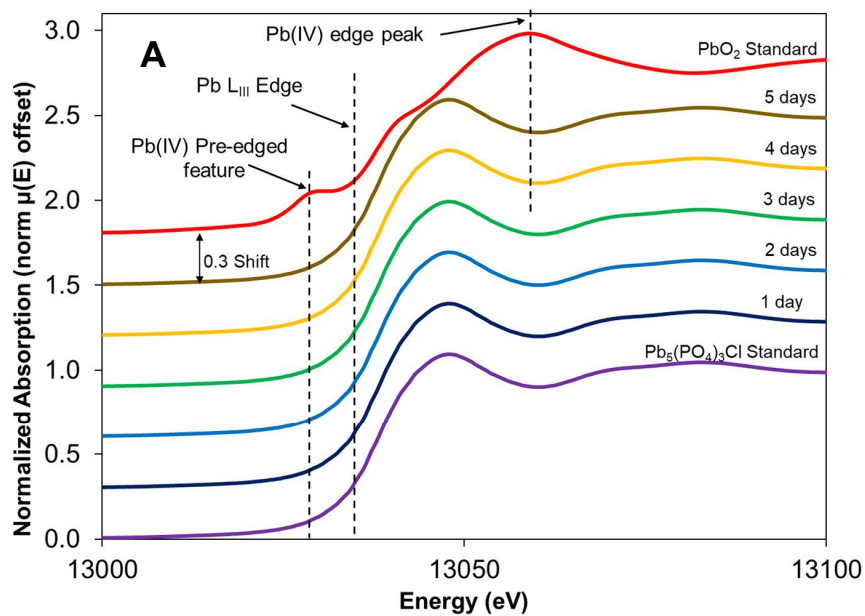
Figure A3 Pyromorphite oxidation by HOCl. $TOTCO_3$ = 10 mM, $[HOCl]_0$ = 4.2 g/L as Cl_2, initial $Cl_2:Pb(II)$=3:1, T=22°C, pH=7. (a) EXAFS. (b) Lead speciation fraction.
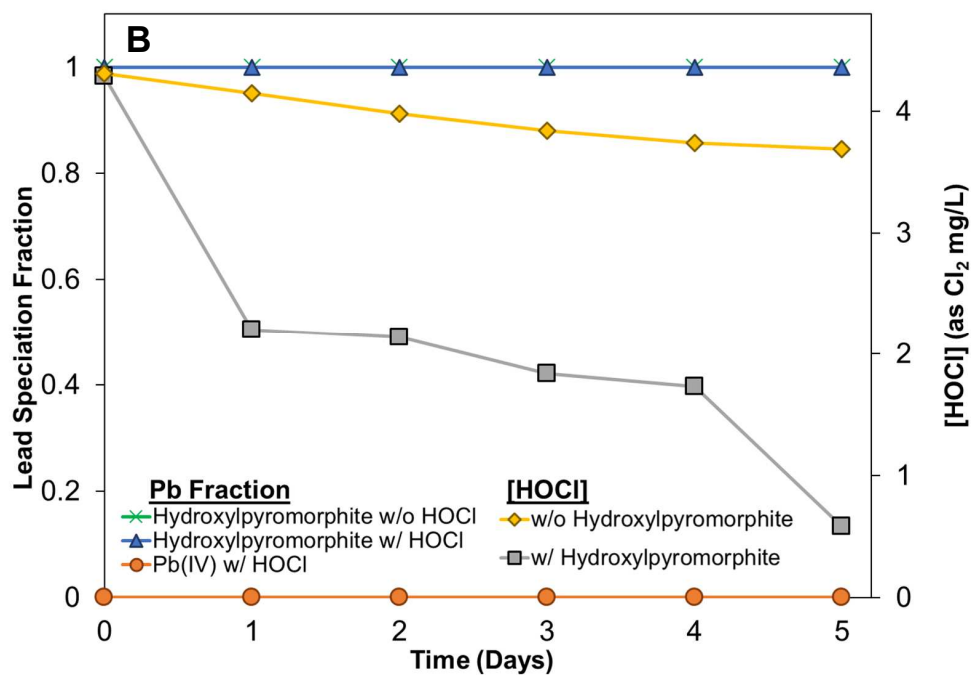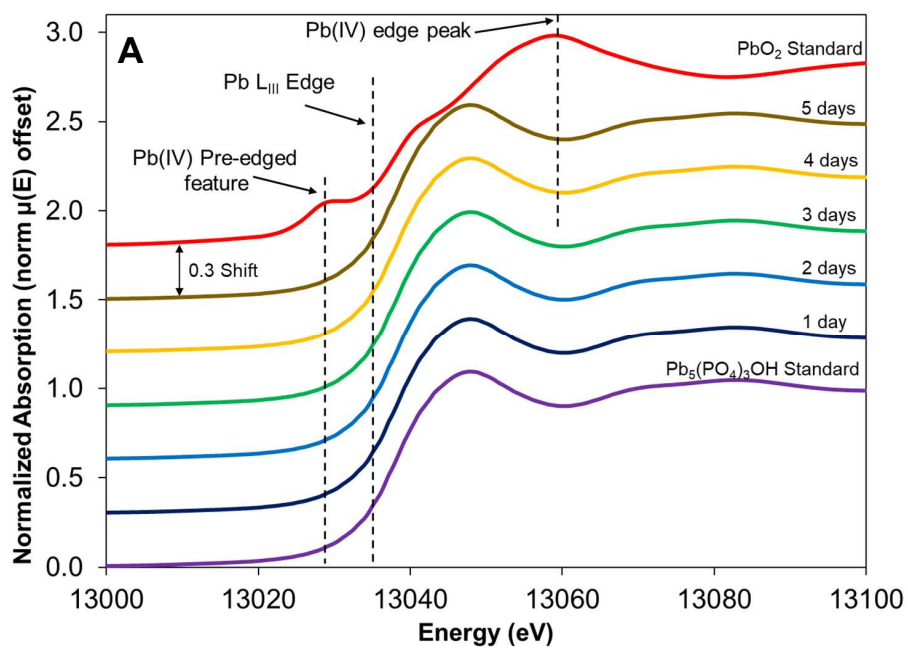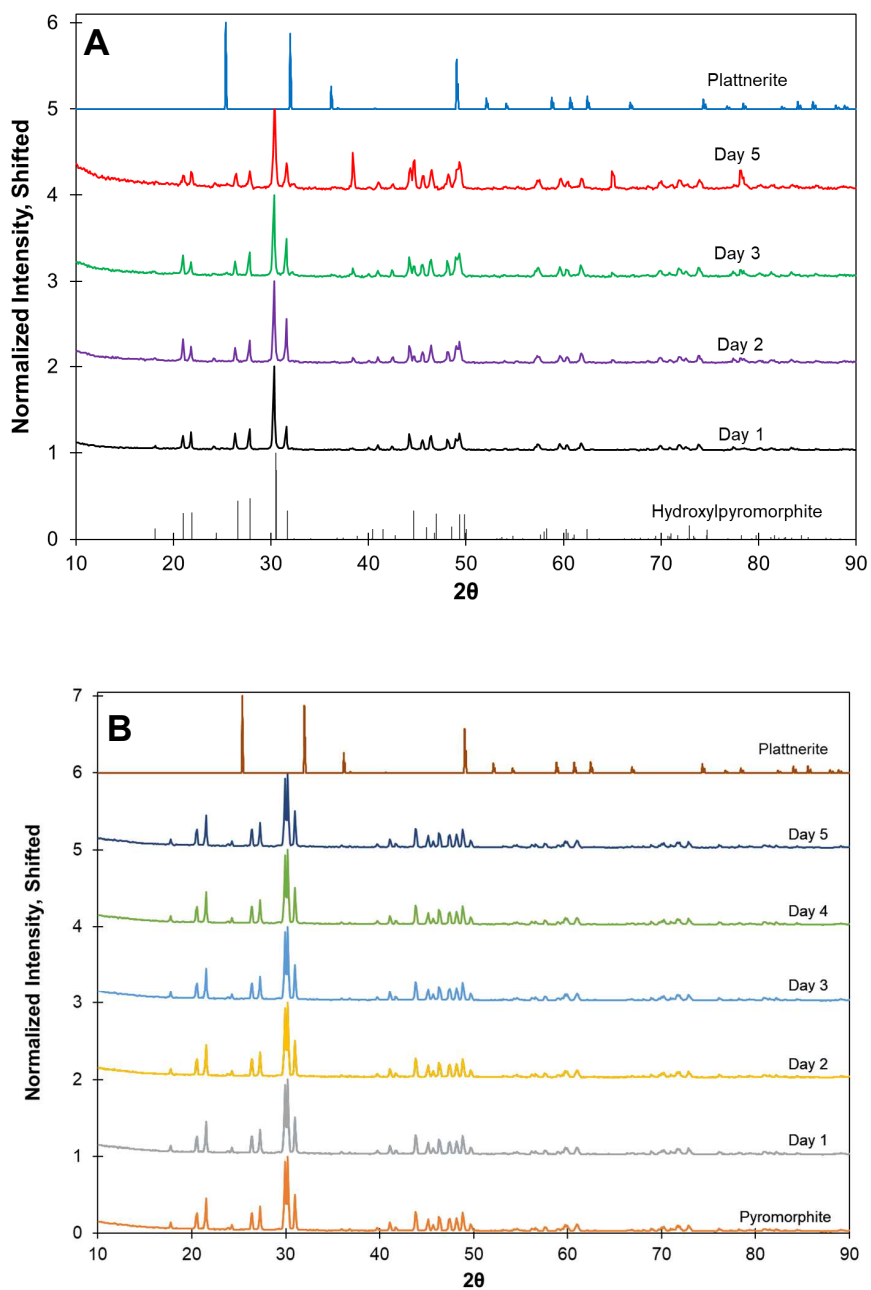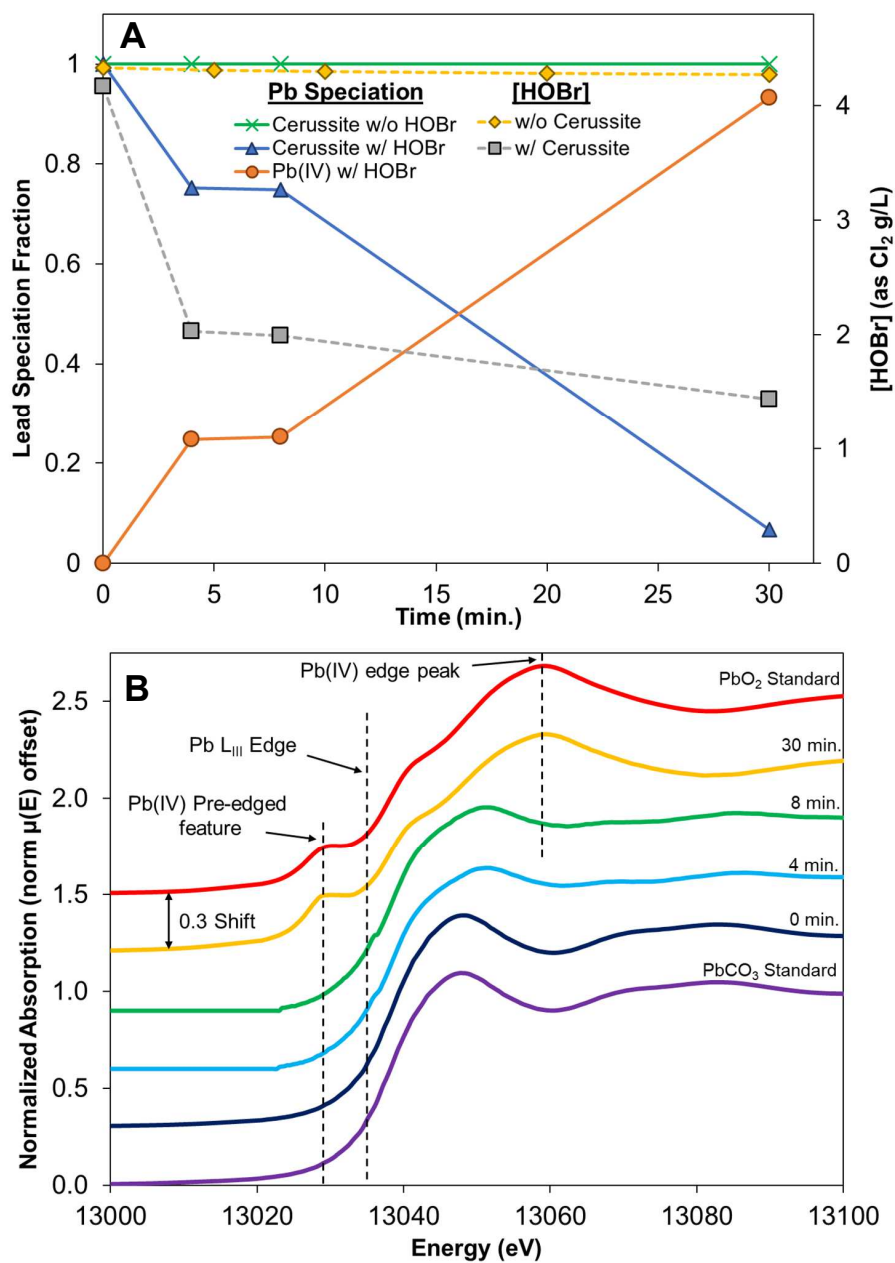
Figure A4 Hydroxylpyromorphite oxidation by HOCl. $TOTCO_3 = 10$ mM, $[HOCl]_0 = 4.2$ g/L as Cl_2, initial $Cl_2:Pb(II)=3:1$, T=22°C, pH=7. (a) EXAFS. (b) Lead speciation fraction
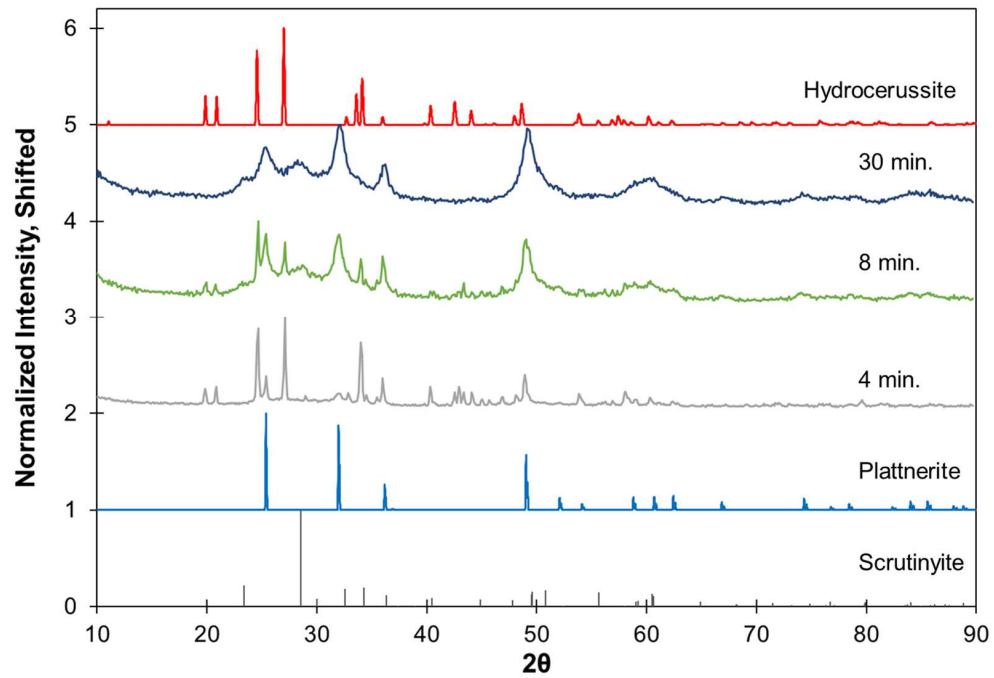
Figure A5 XRD spectra of lead solids during oxidation by free chlorine. $TOTCO_3 = 10$ mM, $[HOCl]_0 = 4.2$ g/L as Cl_2, initial $Cl_2:Pb(II)=3:1$, T=22°C, pH=7. A) Hydroxylpyromorphite B) Pyromorphite.

Figure A6 Cerussite oxidation by HOBr. $TOTCO_3$ = 10 mM, $[HOCl]_0$ = 4.2 g/L as Cl_2, initial Cl_2:Pb(II)=3:1, T=22°C, pH=7. (a) EXAFS. (b) Lead speciation fraction.

Figure A7 XRD spectra of lead solids during cerussite oxidation by free bromine. TOTCO$_3$ = 10 mM, [HOBr]$_0$ = 4.2 g/L as Cl$_2$, initial Cl$_2$:Pb(II)=3:1, T=22°C, pH=7.
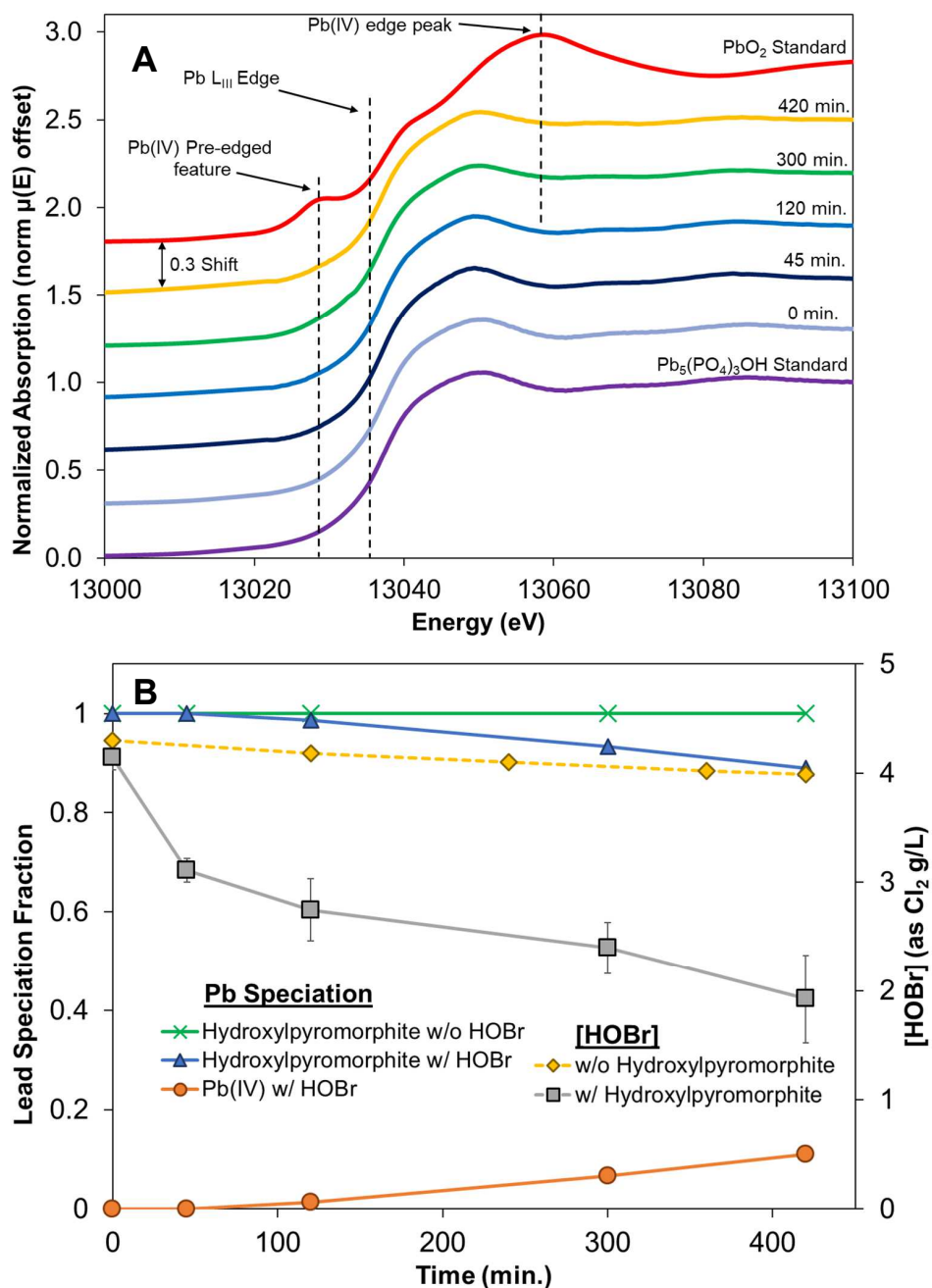
Figure A8 Hydroxylpyromorphite oxidation by HOBr. $TOTCO_3$ = 10 mM, $[HOCl]_0$ = 4.2 g/L as Cl_2, initial Cl_2:Pb(II)=3:1, T=22°C, pH=7. (a) EXAFS. (b) Lead speciation fraction.
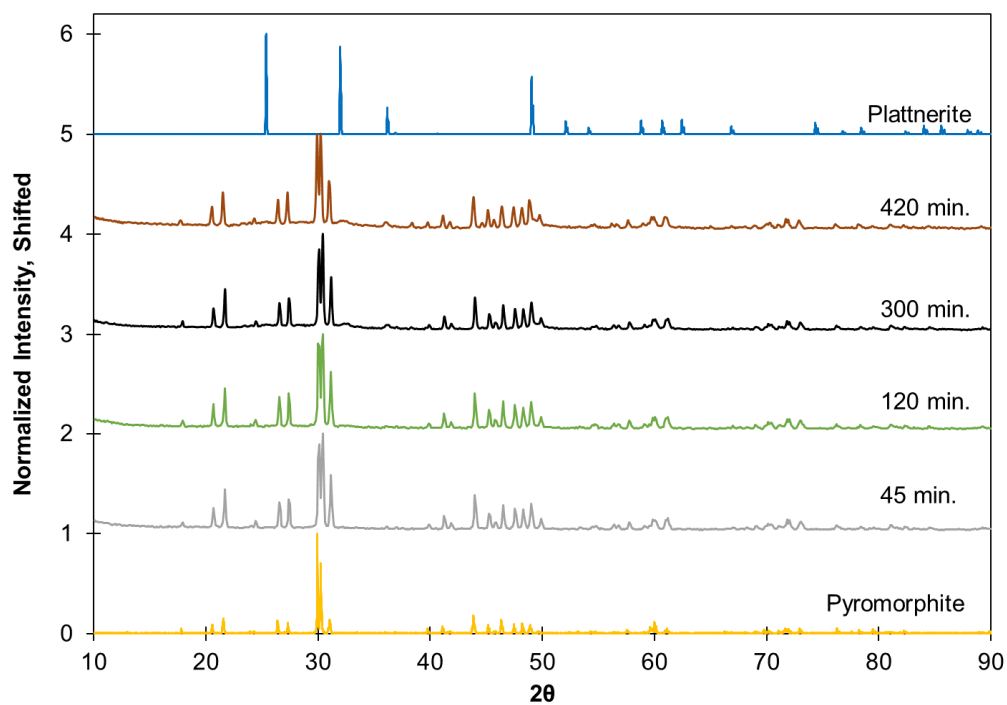
Figure A9 XRD spectra of lead solids during pyromorphite oxidation by free bromine. $TOTCO_3 = 10$ mM, $[HOBr]_0 = 4.2$ g/L as Cl_2, initial Cl_2:Pb(II)=3:1, T=22°C, pH=7.

(^{1}) U.S. Environmental Protection Agency. Optimal corrosion control treatment

evaluation technical recommendations for primary agencies and public water systems.

2016.

(^{2}) U.S. Environmental Protection Agency. Secondary drinking water standards:

Guidance for nuisance chemicals. Available online:

https://www.epa.gov/dwstandardsregulations/secondary-drinking-water-standards-

guidance-nuisance-chemicals